Improvement of Transient Power Sharing Performance in Parallel Converter System and Microgrids

Alhasheem, Mohammed Adel Mohammed Zaki Youssef

Publication date:
2019

Document Version
Publisher's PDF, also known as Version of record

IMPROVEMENT OF TRANSIENT POWER SHARING PERFORMANCE IN PARALLEL CONVERTER SYSTEM AND MICROGRIDS

BY
MOHAMMED ALHASHEEM

DISSERTATION SUBMITTED 2019

AALBORG UNIVERSITY
DENMARK

Improvement of Transient Power Sharing Performance in Parallel Converter System and Microgrids

Ph.D. Dissertation

Mohammed Alhasheem

Dissertation submitted November, 2019

Dissertation submitted: November, 2019

PhD supervisor: Assoc. Prof. Pooya Davari
Aalborg University, Denmark

Co-supervisor: Prof. Frede Blaabejrg
Aalborg University, Denmark

PhD committee: Associate Professor Daniel Ioan-Stroe (Chair)
Aalborg University

Professor Jorma Kyyrä
Aalto University

Team Manager- Power Electronics Alireza Nami
ABB, Sweden

PhD Series: Faculty of Engineering and Science, Aalborg University

Department: Department of Energy Technology

ISSN (online): 2446-1636
ISBN (online): 978-87-7210-533-8

Published by:
Aalborg University Press
Langagervej 2
DK – 9220 Aalborg Ø
Phone: +45 99407140
aauf@forlag.aau.dk
forlag.aau.dk

Simulations included in this dissertation were accomplished using MATLAB® and PLECS® software. For experimental tests, the control system was implemented using dSpace® MicroLabBox DS1202-4 and dSpace® DS1007, which are interfaced by Control Desk®. Power converters used for experimental verifications were Danfoss® VLT FC102 and SEMIKRON® PM50. Finally, this dissertation is typeset using LaTeX ®.

Printed in Denmark by Rosendahls, 2019

Curriculum Vitae

Mohammed Adel Alhasheem

Received the B.Sc. and M.Sc. degrees in electrical and control engineering from the Department of Electrical and Control, Arab Academy for Science, Technology and Maritime Transport, Cairo, Egypt, in 2012 and 2015, respectively. He is pursuing the Ph.D. degree at Department of Energy Technology, Aalborg University, Aalborg, Denmark. He joined the Management and Engineering Department, University of Padua, Italy as a Visiting Scholar, where he focused on several research activities under the supervision of Prof. P. Mattavelli. His current research interests include predictive control for the power converter, microgrids, power quality. Mr. Alhasheem serves as a Reviewer with several journals, including IEEE Transactions on Power Electronics, the IEEE Transactions on Industrial Electronics, the Journal of Emerging and Selected Topics in Power Electronics and IEEE Transactions on Industry Application. He is a member of IEEE and CIGRE where he contributes to several working groups.

Curriculum Vitae

Acknowledgement

Thank you, God, the merciful and the passionate, for giving me the strength and encouragement, especially during all the challenging moments in completing this thesis. I am truly grateful for your exceptional love and grace during this entire journey.

Foremost, I would like to express my sincere gratitude to my advisors Prof. Frede Blaabjerg and Assoc. Prof. Pooya Davari for their continuous support of my PhD study and research, for their patience, motivation, enthusiasm, and immense knowledge. Their guidance helped me in all the time of research and writing of this thesis. I could not have imagined having better advisors and mentors for my PhD study. My sincere thanks also go to Prof. Paolo Mattavelli, for offering me the opportunities in his group and leading me working on an exciting project. I am grateful to all labmates and collaborators I have had the pleasure to work with during this and other related projects.

I am especially indebted to Prof. Rania El-Sharkawy and Prof. Sherif El-Fiki, who have been supportive of my career and life goals and who provided me with fruitful advices and guidance. I owe a great debt to Malena Østergaard for her constant encouragement and help throughout the research period.

Nobody has been more important to me in the pursuit of this project than my family. I want to thank my parents, whose love and guidance are with me in whatever I pursue. They are the ultimate role models. Most importantly, I wish to thank my lovely wife, Sümeyye, who provided unending support. I am particularly grateful for her patience, motivation, and the love that she gave to me during my hard and sleepless days.

Last but not least, I would like to thank my friends and relatives in Denmark and Egypt, who were as a backbone for me during my long journey. Thanks for the memories that we have shared over the past few years and for providing an outlet for my research. Finally, this work would not have

been possible without the financial support of Aalborg University and Arab Academy for Science, Technology and Maritime Transport. I am very grateful to all those at the secretary offices, who were always so helpful and provided me with their assistance throughout my dissertation.

Mohammed Alhasheem
Aalborg, Denmark

Abstract

Over the past couple of decades, a rapid penetration of distributed generators (DGs) such as photovoltaic (PV), energy storage systems (ESSes), wind turbines and others has occurred in the electrical power system. However, since the legacy grid has not been initially designed to accept such DGs, a solution to simplify the integration of DG units to the main grid through a so-called microgrid (MG) entity was proposed. MGs are one of the key technologies that will enable penetration of renewable energy sources (RES) in the power system. By aggregating multiple RES with distributed adaptive loads results in achieving much higher flexibility than individual operation. In this context, MGs can be used to provide different types of ancillary services e.g. voltage support. Also, in the case of an outage or low power quality of utility mains, they can seamlessly disconnect and continue to supply the loads with high-quality power in stand-alone mode.

It is usually necessary to establish an alternating current (AC) MG structure since a vast majority of conventional loads require AC power supply. Therefore, power electronics converters serve as interfaces between the direct current (DC) sources and the AC parts. Among different power converters, voltage source converters (VSCs) will be intensively studied as it will serve as the interface/interlink to the MG. A challenge to be overcome in the MG technology is to realize the operation of parallel-connected converters with good load sharing ability in both steady-state and transient conditions. The conventional principle of controlling these converters is based on cascading linear control loops. However, such a structure has inherent limitations such as slow response and sensitivity to control parameter settings.

This Ph.D. project proposes an alternative way of designing the MG control structure. It takes advantage of the fast evolution of digital signal processors, which is a platform for the integration of control algorithms for power converters and drive applications. The key idea is to use that raw processing power to embed all the inner control loops within a single algorithm that

takes into account the model of the converter and its associated filter. In that sense, the principle of using a discrete model of the voltage source converter with an associated filter to predict its future behaviour for all possible control inputs, and consequently applying the one that minimizes a programmed cost function (CF) at every sampling time will be deployed. This kind of control strategy is referred to as the finite control set (FCS) model predictive control (MPC). Due to its flexibility and inherently fast response, such principle has been widely and successfully applied to individual converters in applications characterized by a high electromotive force, e.g. motor drives applications. However, this method has not fully explored and investigated in MG applications. This project aims to fill this gap both by theoretical research and experimental demonstration, which will be developed to study various aspects of the problem. Moreover, investigating the performance of the proposed control structure in parallel operation is one of the main goals of this project. Also, the effect on power quality has been addressed and the feasibility of applying FCS-MPC control strategy is further studied through efficiency analysis. Based on that, improved control strategies have been proposed and presented in this thesis to ensure high quality and fast operation of the future MGs.

Finally, this thesis seeks to answer some questions, which are related to the performance of different control strategies of a typical VSC to be employed in the MG operations. Also, the study seeks to leave the door open for other researchers to increase the feasibility of the proposed solutions and provide extra investigations.

Abstrakt

I løbet af de sidste par årtier er der sket en hurtig udbredelse af distribuerede energi kilder (DG'er) såsom solcelle-systemer (PV), energilagringssystemer (ESSes), vindmøller o.a. i det elektriske energi-system. Da nettet ikke oprindeligt er blevet designet til at acceptere så mange generatorer, er der imidlertid foreslået en løsning til at forenkle integrationen af DG-enhederne til hoved el-nettet gennem et såkaldt mikro-net (MG). MG'er er en af de nye lovende teknologier, der gør det muligt at integrere vedvarende energikilder (RES) i el-systemet mere effektivt. Ved at aggregere (sammenlægge) flere RES sammen med distribuerede dynamiske belastninger er det muligt at opnå langt højere fleksibilitet end ved individuel drift af enhederne. I den sammenhæng kan MG'er bruges til at levere forskellige typer af ekstra tjenester til el-nettet, såsom spændings- og frekvens-støtte. I tilfælde af strømafbrydelse eller lav strømkvalitet på hoved el-nettet, kan MG'erne problemfrit afbryde forbindelsen og fortsætte med at forsyne belastningerne med høj kvalitet af spændingen (MG'en arbejder i stand-alone). Det er som oftest nødvendigt at etablere en vekselspændings-baseret (AC) MG-struktur, da langt de fleste konventionelle belastninger kræver vekselstrøm.

Derfor tjener effektelektroniske omformere, som grænseflade imellem jævnspændingskilder (DC) og vekselstrømmen i el-nettet. Blandt de forskellige typer effektkonvertere studeres for øjeblikket spændingskilde-konvertere (VSC'er) intensivt, da de er de mest vel-egnede. Den væsentligste udfordring, der skal overvindes i MG-teknologien, er at realisere driften af parallelle tilsluttede konvertere, som har en god evne til at fordele belastningen imellem sig under både normal drift og kortvarige udfald. Det konventionelle princip for styringen af disse konvertere er baseret på såkaldte kaskade baseret lineær kontrol sløjfer (loops). Imidlertid har en sådan struktur indbyggede begrænsninger, såsom langsom respons og større følsomhed over for kontrol parameterindstillingerne Derfor foreslår dette ph.d. projekt en alternativ måde at designe MG-kontrol strukturen på. Det drager fordel

af den hastige udvikling af digitale signalprocessorer der bliver billigere og bedre og som er en platform for integrationen af kontrol-algoritmerne til omformer-teknologien i et mikro-net.

Hovedidéen er at bruge beregningsskraften i moderne DSP'ere til at integrere alle de indre kontrol sløjfer i konverteren til en enkelt algoritme, der tager højde for både konverterens modeller og det tilhørende filter. I praksis anvendes en diskret model af konverteren med dens tilknyttede filter til at forudsige dens fremtidige opførsel for alle mulige kontrolindgange analyseres, for så endelig at anvende den, der minimerer en omkostningsfunktion (CF) i hvert samplingstidspunkt. Denne type kontrolstrategi omtales som " finite control set" (FCS) model prediktiv kontrol (MPC). På grund af metodens fleksibilitet og sin naturlige hurtige reaktion, er dette princip blevet anvendt med succes på individuelle konvertere i mange applikationer, såsom nettilslutninger af vedvarende energi-kilder og til motorstyringer. Imidlertid har denne metode ikke set nogen anvendelse i autonome og parallelle tilslutninger, hvilket er karakteristiske træk for MG'er. Dette projekt udfylder dette hul både ved teoretiske analyser og eksperimentelle analyser, hvor forskellige aspekter af den foreslåede metode er undersøgt. Derudover er performancen af den foreslåede kontrolstruktur i parallel drift også et af hovedformålene at undersøge i dette projekt. Virkningsgrad og strømkvalitet under normal og unormal nettilstand er desuden også undersøgt. Endelig er der i dette projekt blevet foreslået og præsenteret flere forbedrede kontrol strategier som sikrer høj kvalitet og god performance af de fremtidige MG'er.

Thesis Details

Thesis Title:	Improvement of Transient Power Sharing Performance in Parallel Converter System and Microgrids
PhD Student:	Mohammed Alhasheem
PhD Supervisors:	Prof. Frede Blaabejrg, Aalborg University Assoc. Prof. Pooya Davari, Aalborg University

The main body of this thesis consists of the following papers:

Publications in Refereed Journals

J1 **M. Alhasheem**, A. Abdelhakim, F. Blaabjerg, P. Mattavelli and P. Davari ''Model Predictive Control of Grid Forming Converters with Enhanced Power Quality'' (under revision at editor's request"), IEEE Access, (2019).

J2 **M. Alhasheem**, F. Blaabjerg, P. Mattavelli , and P. Davari, Harmonics Mitigation Utilizing Active Power Filter Based On Predictive Control under Unbalanced Grid Voltage, ", IET Power Electronics, submitted, (2019).

J3 **M. Alhasheem**, F. Blaabjerg, and P. Davari, ''Performance Assessment of Grid Forming Converters Using Different FCS- MPC Algorithms', Appl. Sci. 2019, Vol.9(17), 3513;

Publications in Refereed Conferences

C1 **M. Alhasheem**, T. Dragicevic , F. Blaabjerg , and P. Davari "Parallel Operation of Dual VSCs Regulated by FCS-MPC Using Droop Control Approach" in Proc. of European Conference on Power Electronics and Applications, 2018, pp. P.1-P.10.

C2 R. Heyderi , **M. Alhasheem**,T. Dragicevic and F. Blaabjerg" Model Predictive Control Approach for Distributed Hierarchical Control of VSC-

based Microgrids" in Proc. of European Conference on Power Electronics and Applications, 2018, pp. P.1-P.8.

C3 **M. Alhasheem**, A. Abdelhakim, T. Dragicevic, L. Dalessandro and F. Blaabjerg "Performance assessment of the VSC using two model predictive control schemes" in Proc. of IEEE Applied Power Electronics Conference and Exposition (APEC), 2018, pp. 450-457.

C4 **M. Alhasheem**, T. Dragicevic, M. Rivera and F. Blaabjerg "Losses evaluation for a two-level three-phase stand-alone voltage source converter using model predictive control" in Proc. of IEEE Southern Power Electronics Conference (SPEC), 2017, pp. 1-6.

C5 **M. Alhasheem**, T. Dragicevic, and F. Blaabjerg, "Evaluation of multi predictive controllers for a two-level three-phase stand-alone voltage source converter" in Proc. of IEEE Southern Power Electronics Conference (SPEC), 2017, pp. 1-6.

C6 T. Dragicevic, **M. Alhasheem**, M. Lu, and F. Blaabjerg "Improved model predictive control for high voltage quality in microgrid applications" in Proc. of IEEE Energy Conversion Congress and Exposition (ECCE), 2017, pp. 4475-4480.

Book Chapters

B1 S Peyghami, **M. Alhasheem**, F Blaabjerg – "Power Electronics-Microgrid Interfacing" IET Press, on the book Variability, Scalability and Stability of Microgrids, 2019.

This dissertation has been submitted for assessment for the Ph.D. degree fulfilment. The thesis is a summary of the outcome from the Ph.D. project, which is documented based on the above publications. Parts of the results are used directly or indirectly in the extended summary of the thesis. The co-author statements have been made available to the assessment committee and are available at the Faculty of Engineering and Science, Aalborg University.

Mohammed Alhasheem
Aalborg University, November 4, 2019

Contents

List of Figures

List of Tables

Part I

Report

Chapter 1

Introduction

1.1 Background

Microgrid (MG) concept was originally proposed in 2002, as a building block of the future low voltage distribution systems and introduction of distributed generation (DGs). Several power converters are typically connected in parallel to form an AC MG. This is done for several reasons. For instance, MGs serve as an alternative power source utilizing unconventional power sources while supply power to the critical loads in the main grid. The parallel operation provides redundancy and high reliability, which is often required in mission critical applications. Moreover, in some cases, it is more economically feasible to split the power into several converters and then use low rating power devices to maximize the overall system efficiency.

The conventional way of realizing the power converters control structure in MGs is through hierarchically organized linear control loops and a pulse width modulator. However, in practice, this control method suffers from several practical limitations. Firstly, the accuracy of power and reactive power control of a given converter depends on the nature (X/R ratio) of the line between the converter and the bus to which it is connected. Since this nature cannot explicitly be known, and can indeed change considerably during the various operating conditions, a virtual impedance approach can be deployed to fix the effective impedance seen by the converter. However, in a classical approach as also mentioned in [1], a separate virtual impedance loop needs to be implemented for each given frequency. Hence, the linear control structure may become very complex when sharing the power among nonlinear loads. Moreover, accurate power sharing in transient periods cannot be guaranteed. Secondly, a cascaded linear structure inherently introduces a low-pass filtering behaviour of the overall control system where the dom-

inant time constant tends to rise by an order of magnitude with every loop. Finally, as the converters normally have an *LC* filter installed at the output, there exists a dynamic coupling between the inductor current and capacitor voltage that is cumbersome to cancel due to the presence of computational and PWM delays [1–3]. Furthermore, there are numerous challenges around developing controllers for power converters and modules to support high-performance applications. Each converter can do the function of interfacing the DGs to the legacy MG. Since the legacy distribution grid was not initially designed to accept such units, they could also introduce some challenges to its operation such as inverse power flow, voltage amplitude deviations and unbalances, harmonic distortion, and resonance problems in the low voltage grid [4].

Also, with the proliferation of nonlinear power electronics loads, the harmonic penetration phenomenon has become very disturbing in microgrid operations. Harmonic currents produced by power electronics converters, rectifiers, electronic power supplies, adjustable-speed motor drive controllers, and battery chargers have been responsible for the rise in power quality problems. Due to the simplicity and low cost of passive power filters, they have been the solution to the mentioned problems for a long time. Many disadvantages were posed by using passive filters such as large size and a possible series or parallel resonance with the system impedance. Active power filters (APFs) can introduce power quality improvement by injecting currents into the grid and in the opposite phase to the distorting harmonics. In that way, harmonics are reduced by superposition. Specifically, a shunt active power filter (SAPF) has become the most popular active filter for harmonics mitigation. In general, the control of an active filter requires fast dynamic performances and that represents a challenging control issue. High control bandwidth may not be able to be addressed by applying conventional linear control strategies. However, several linear control techniques have been proposed to fulfil the high bandwidth requirements. For instance, PI controllers are introduced but still unable to provide a satisfactory regulation performance [5]. Other control schemes aimed to improve the tracking accuracy by using multiple related synchronous reference frames and obtain a satisfactory tracking performance [6]. That structure increases the complexity and effort of controller tuning. To avoid multiple reference frame transformations, proportional resonant controllers may be used [7]. Finally, dead-beat control strategies [8] have also been considered in order to fulfil the high bandwidth requirements.

Recently, finite control set model predictive control (FCS-MPC) has become a popular strategy for the control of power converters. Due to its flexibility and inherently fast response, FCS-MPC has been successfully applied to grid-connected and stand-alone converters, as well as to electrical drives [9]. The main drawback of FCS-MPC is its computational intensity that especially becomes critical in power electronics applications, which are

characterized by relatively small sampling times. This issue essentially prohibits an online evaluation of all possible switching configurations for more than one sampling period ahead, since the number of computations rises exponentially with every step [9]. Therefore, there is a need to develope FCS-MPC to have good power quality with less computational burden in order to take the advantages of its flexibility and fast response.

In general, predictive control can be considered as any algorithm that uses a model of the system to predict its future behaviour and selects the most appropriate control action based on an optimality pre-programmed criterion. The predictions are evaluated through a pre-programmed cost function (CF), and then, the sequence that minimizes the CF is chosen in order to obtain the future control action. The CF is a representation of the control objectives that are usually related to making the variables following the references. Further, when two or more objectives must be achieved simultaneously, they can be combined in a sum of squared error terms as demonstrated in the following:

$$\begin{aligned} g_o = &(X_\alpha(k+1) - X_\alpha^*(k))^2 + (X_\beta(k+1) - X_\beta^*(k))^2 + \lambda_a(Y_\alpha(k+1) - Y_\alpha^*(k))^2 \\ &+ Y_\beta(k+1) - Y_\beta^*(k))^2 + ... + \lambda_b(N_\alpha(k+1) - N_\alpha^*(k))^2 + (N_\beta(k+1) - \\ &N_\beta^*(k))^2. \end{aligned} \tag{1.1}$$

Where X, Y, N are different control objectives and λ_a, λ_a are weighting factors, which are used to control the importance of each objective. If these objectives have the same nature, such as direct and quadrature component of the current or the active and reactive power, they can be added directly. If the variables have different natures, such as magnetic flux and torque or voltages and currents, they must be added including a normalization. In both cases, a weighting factor can be multiplied by these terms to give a relative importance to one or another [10]. However, CF based on one-step prediction horizon becomes problematic when controlling higher order plants (as is the case with *LC* filter) due to couplings between different state variables. In this thesis, a solution is proposed, which explicitly deals with the dynamic coupling between the inductor current and capacitor voltage, allowing the usage of a single-step prediction horizon for effective voltage control of the *LC* filter in MG applications. The CF includes terms that improve particular features in each converter such as to minimize the common-mode voltage, to reduce the switching frequency, to minimize the losses as shown in Fig. 1.1. This feature gives high flexibility to predictive control, which is tough to be achieved by using linear controllers that require additional and complex control structures or modifications to the modulation [10]. In that sense, MPC needs a high amount of calculations in order to solve the optimization problem online. One solution to reduce the computational time is to con-

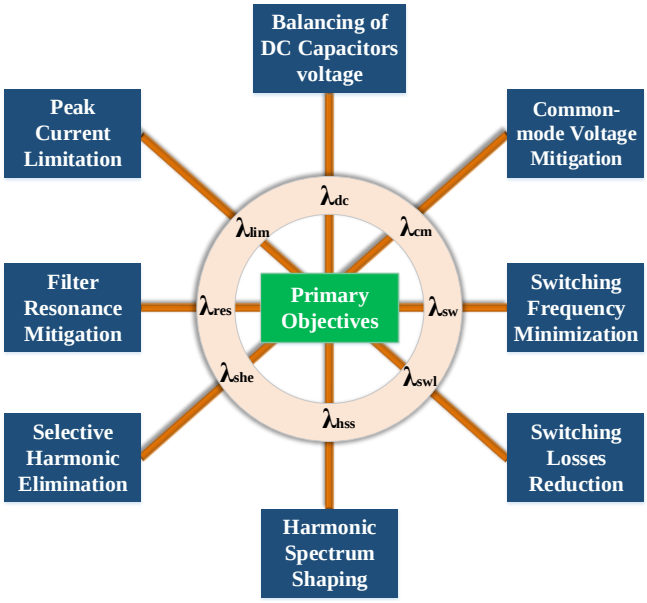

Fig. 1.1: Overview of utilized cost functions in power electronic converters including primary and secondary control objectives.

sider or apply offline optimization approaches [11]. Another solution is to use generalized predictive control (GPC), where the optimization is solved analytically. Nevertheless, in GPC, it is very difficult to include system constraints and non-linearities. The ideal approach to implement MPC for power converters and adjustable speed drives is to take advantage of the inherent discrete nature of the power converter [12]. Since power converters have a finite number of switching states, the MPC optimization problem can be simplified and reduced to the prediction of the system behaviour only for those possible switching states. This approach is known as finite control set model predictive control [13, 14].

Finally, MGs, as shown in Fig. 1.2, are recognized as one of the key technologies that enable high penetration of renewable energy sources. As discussed before, they can provide ancillary services and in case of an outage or low power quality of utility mains, MGs can be disconnected from the utility mains and continue to operate in stand-alone mode. However, the system stability issues in an MG are well known and have been investigated by many researchers recently, focusing on particular aspects, types of MG, the control topology, and also the network parameters, etc. The stability in an MG largely depends on the control strategy of the VSCs [9, 15]. Therefore, grid forming VSC needs to be able to regulate the voltage of the common bus to a specified amplitude and frequency without support of the overhead

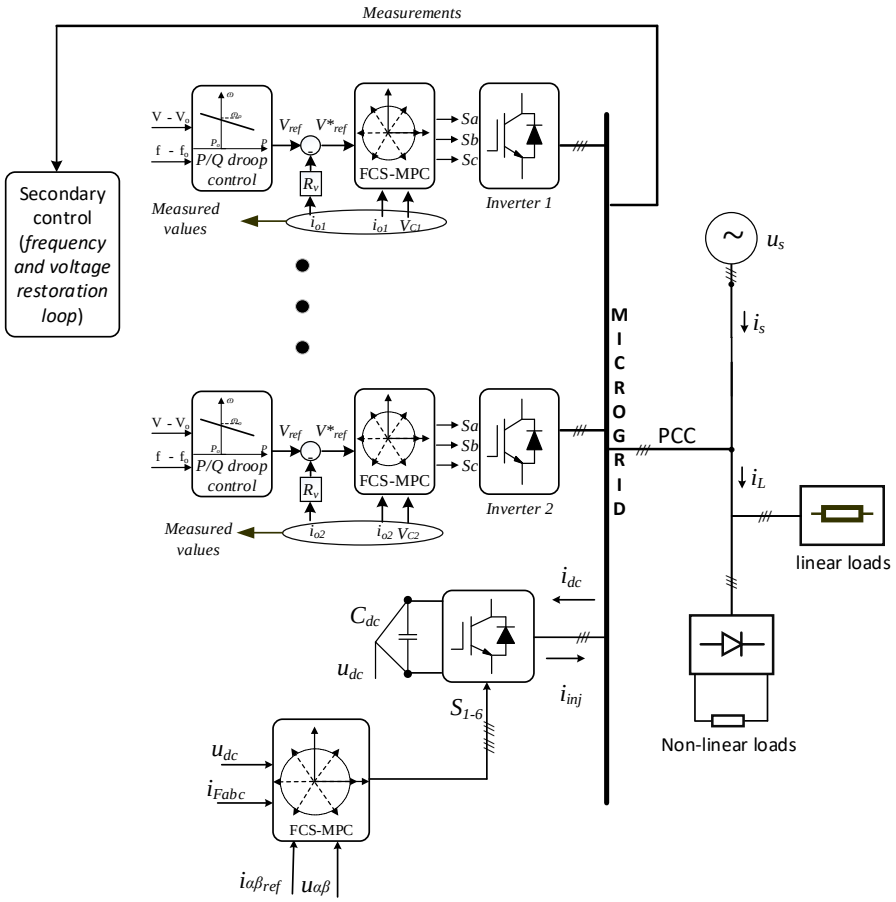

Fig. 1.2: The proposed control structure of voltage source converters connected to a microgrid.

system [16]. By doing so, it can also synchronize with the utility voltage in order to seamlessly connect with it, and inject power. In that case, VSC can be called a grid-following converter. Subsequently, when more VSCs are connected in parallel (as in Fig. 1.2), reference voltage amplitude and frequency of each VSC is not fixed but needs to be adapted in order to ensure a proper power sharing among different modules and the grid. Those VSCs cooperatively regulate the voltage and they are called grid-supporting components.

This project aims to address applying the FCS-MPC solution in MG applications and considering the current challenges in both stand-alone and grid-connected operations. That will enable to take the advantages of its flexibility and fast response. Also, to avoid using linear control loops and embed the hierarchical control structure within a single control unit. Moreover, this

solution will be applied to active power filters as well. Worth to mention that typical voltage source converters (VSCs) are used in this study.

1.2 Project motivation

As the world moves towards renewable and green energy generation and acts to counter climate change, MGs offer a wide range of benefits, which can provide assistance in terms of the environmental benefits, economic advantages and increased efficiency. Moreover, MPC is an interesting and intuitive control method for power electronics converters. However, still dynamic operations are not clear and therefore it is important to analyze this aspect in both islanded and grid-connected modes. Pulsed loads such as radars, sonars and electric vehicle chargers (EV) can cause a step change during the operation and can affect the microgrid operation. Having the FCS-MPC algorithm will enable the converter to compensate for the immediate requirement of voltage with fast response. Therefore, controlling the power converters with FCS-MPC method results in better transient performance. Similarly, a load step-change will occur in the case of multiple converters, which are connected to the grid. The fast response will be achieved by using the FCS-MPC control algorithm and ensure a sharing accuracy for the parallel configuration. Hence, connecting multiple converters regulated by FCS-MPC method results in an increase in the load sharing accuracy and maintain the dynamic performance. In that context, a clearer picture of the robustness of the controller is needed. Therefore, a set of analysis and different approaches are needed to validate the robustness on the stability of the MG in both standalone and grid-connected systems. For such configurations, also power quality needs to be addressed. In that case, a simple and effective control structure is required to enhance the power quality. Therefore, shunt active power filter (SAPF) regulated by FCS-MPC has been used and based on a single objective cost function. That will also provide a fast response in compensation of harmonics and unbalanced grid voltages. Besides, it would be interesting if that goal can be achieved with a less complex system compared to the existing techniques.

1.3 Project hypothesis and objectives

The main hypothesis is that FCS-MPC can provide a faster transient response, more robustness to parameter variation and inherent stability in all operating modes comparing to the classical control techniques and that can all be analytically or experimentally proved too.

The objectives of this Ph.D. project are to answer for coming research questions:

- ☐ How will the FCS-MPC improve the performance of one stand-alone converter in transient and steady state when both feeding linear and non-linear loads?
- ☐ How is the performance of FCS-MPC compared to the existing classical control techniques?
- ☐ How will the FCS-MPC improve the performance in a paralleled converter system (or an MG) in both linear and non-linear loads?
- ☐ How can the FCS-MPC connect the converter systems to the legacy grid?
- ☐ Can we guarantee the performance of FCS-MPC regulated converters?
- ☐ How can the FCS-MPC improve the performance of the active power filters?

1.4 Thesis outline

The outcome of the Ph.D. project is documented in this Ph.D. thesis based on the collection of papers published during the Ph.D. study. The document is structured in two main parts: Report and Appended papers. The thesis structure is illustrated in Fig. 1.3, and providing a guideline for how the content in the Report is connected to the Publications. In the Report, a brief summary of the research conducted during the Ph.D. study is presented, where the main results are based on the selected Publications. The Report is organized into six chapters. In Chapter 1, the introduction of the Ph.D. thesis is provided, where the background of the research topic and the objectives of the Ph.D. study are discussed. Then, the following two chapters deal with the benchmarks and performance of the studied topology utilizing conventional and improved predictive control schemes. The main focus of Chapter 2 is giving an overview of the control strategies used in the thesis. In Chapter 3, the performance of the selected control strategies of grid-forming converters is discussed and compared to the conventional and improved MPC schemes. The results are validated with simulation and experiments. Also, Chapter 3 addresses the power quality, efficiency, and switching frequency challenges, where different techniques to control the switching frequency are implemented and investigated. The chapter includes further analysis, modelling, and mitigation of the harmonics. In Chapter 4, a control structure based on FCS-MPC is proposed for an active power filter where the transient performance and power quality are considered. Further, compensation of the unbalance grid voltage using the proposed structure is also analyzed. The performance of the proposed control strategy is compared to one of the conventional strategies, which is using space vector control. Then, in Chapter 5,

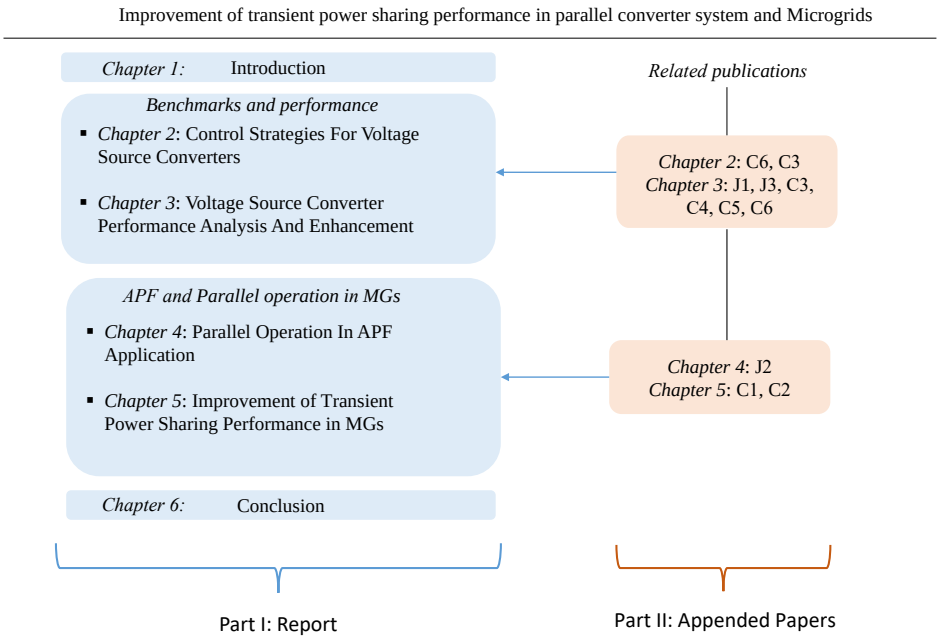

Fig. 1.3: Thesis structure and related papers of each part.

possible solutions to enhance the operation of MGs through the integration of the grid forming converters are discussed. Finally, concluding remarks and the main contributions in this Ph.D. thesis are summarized in Chapter 6 where also the future research perspectives are outlined.

1.5 List of publications

The research outcomes during the Ph.D. study have been disseminated in several forms as listed in the following. Most of them are used in the Ph.D. thesis as previously listed.

Publications in refereed journals

J1 **M. Alhasheem**, A. Abdelhakim, F. Blaabjerg, P. Mattavelli and P. Davari ''Model Predictive Control of Grid Forming Converters with Enhanced Power Quality" (under revision at editor's request"), IEEE Access, (2019).

J2 **M. Alhasheem**, F. Blaabjerg, P. Mattavelli , and P. Davari, Harmonics Mitigation Utilizing Active Power Filter Based On Predictive Control under Unbalanced Grid Voltage, ", IET Power Electronics, submitted, (2019).

J3 **M. Alhasheem**, F. Blaabjerg, and P. Davari, ''Performance Assessment of Grid Forming Converters Using Different FCS- MPC Algorithms', Appl. Sci. 2019, Vol.9(17), 3513;

Publications in refereed conferences

C1 **M. Alhasheem**, T. Dragicevic , F. Blaabjerg , and P. Davari "Parallel Operation of Dual VSCs Regulated by FCS-MPC Using Droop Control Approach" in Proc. of European Conference on Power Electronics and Applications, 2018, pp. P.1-P.10.

C2 R. Heyderi , **M. Alhasheem**,T. Dragicevic and F. Blaabjerg" Model Predictive Control Approach for Distributed Hierarchical Control of VSC-based Microgrids" in Proc. of European Conference on Power Electronics and Applications, 2018, pp. P.1-P.8.

□ R. Heyderi , **M. Alhasheem**, S. Peyghami, T. Dragicevic and F. Blaabjerg Publication for scientific paper" Unified Power sharing Control in Hybrid AC/DC Microgrids Employing Synchronous Machines Principle" in Proc. of European Conference on Power Electronics and Applications, 2018, pp. P.1-P.8.

C3 **M. Alhasheem**, A. Abdelhakim, T. Dragicevic, L. Dalessandro and F. Blaabjerg "Performance assessment of the VSC using two model predictive control schemes" in Proc. of IEEE Applied Power Electronics Conference and Exposition (APEC), 2018, pp. 450-457.

C4 **M. Alhasheem**, T. Dragicevic, M. Rivera and F. Blaabjerg "Losses evaluation for a two-level three-phase stand-alone voltage source converter using model predictive control" in Proc. of IEEE Southern Power Electronics Conference (SPEC), 2017, pp. 1-6.

C5 **M. Alhasheem**, T. Dragicevic, and F. Blaabjerg, "Evaluation of multi predictive controllers for a two-level three-phase stand-alone voltage source converter" in Proc. of IEEE Southern Power Electronics Conference (SPEC), 2017, pp. 1-6.

C6 T. Dragicevic, **M. Alhasheem**, M. Lu, and F. Blaabjerg "Improved model predictive control for high voltage quality in microgrid applications" in Proc. of IEEE Energy Conversion Congress and Exposition (ECCE), 2017, pp. 4475-4480.

Book chapters

B1 S Peyghami, **M. Alhasheem**, F Blaabjerg – "Power Electronics-Microgrid Interfacing" IET Press, on the book Variability, Scalability and Stability of Microgrids, 2019.

Chapter 2

Control Strategies For Voltage Source Converters

This chapter provides an overview of the utilized control strategies throughout the entire PhD research. The chapter discusses conventional stationary and synchronous reference frame including carrier-based pulse width modulation technique as a basis for a comparative study with respect to FCS-MPC. Also, both conventional FCS-MPC and improved FCS-MPC schemes are discussed and their cost functions are provided.

2.1 Background

As a key enabling technology to control the power in various applications, power electronic systems play an essential role in realizing the different control strategies. Conventionally, a carrier-based (CB) algorithm is implemented to control the voltage source power converters to deliver the captured power into the grids or to consumers. The linear control structure becomes complicated when sharing or feeding the power among linear or nonlinear loads. In order to realize a simple control structure of the grid-connected power converters, the linear control structure needs to be replaced with a more flexible and straightforward algorithm, which can meet the grid requirements and required standards. Specifically, the desired control structure should have similar steady-state performance, such as the traditional control strategy or even better. Besides, it should have the ability to act fast in case of frequent load changing. This fast behaviour can be achieved by regulating the control targets without the need for hierarchical control loops or parameters tuning effort. This problem can be solved using model predictive control (MPC) strategies as also discussed in the introduction.

Following the above discussion, carrier controllers based on pulse width modulation (PWM) or space vector modulation (SVM) and FCS-MPC control solutions based on conventional or improved methods will be discussed in this chapter. The circuit topology, as shown in Fig. 2.1, is considered in the implementation and in the presented results. The voltage source converter (e.g., DC–AC converter) is employed to convert DC to AC and deliver power either into the grid or to the different loads [17, 18]. In the following, carrier-based control algorithms in the stationary and synchronous reference frame are discussed. Bearing in mind that the discussion refers to some implemented works which are developed by other researchers. Their research outlet has been used to benchmark conventional and improved FCS-MPC. Also, the discussed algorithms have been simulated and validated experimentally to build up an understanding and awareness of each algorithm.

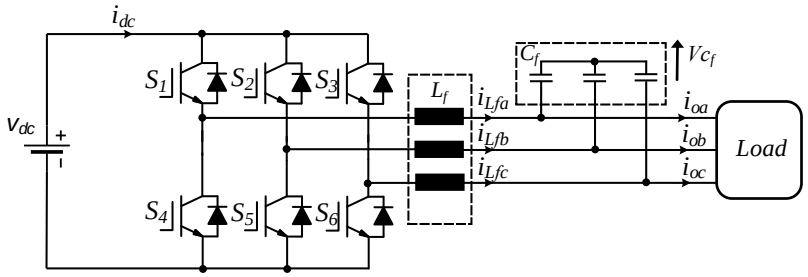

Fig. 2.1: The power circuit schematic of the VSC.

2.2 Conventional control schemes

2.2.1 Carrier-based sinusoidal pulse width modulation (CB-SPWM)

The conventional way of realizing overall VSC control structure is by using organized linear loops utilizing PWM. Inaccurate design of the inner loops may degrade the performance of the whole control system. According to Kerkman [19], it is desirable that any voltage or current regulator can achieve zero steady-state error, have a high bandwidth as much as possible, and accurately track the input references. Discussed herein is the implementation of the inner regulator, which is based on proportional resonant (PR) controllers in the stationary reference frame, as explained in details in [20, 21]. In this way, α and β quantities are decoupled, while in the synchronous reference frame the implementation of the decoupling techniques is required since the states of d and q axis are not independent [22, 23]. Also, using the $\alpha\beta$ frame

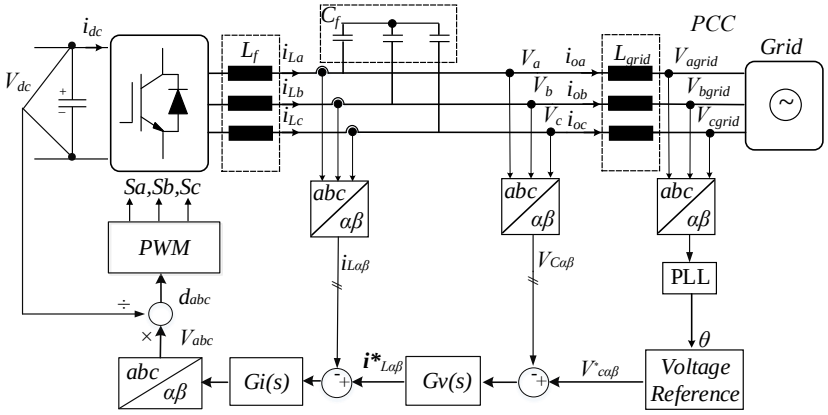

Fig. 2.2: The power circuit and classical control structure of the used inverter for microgrid applications.

gives another advantage, which is a low computational burden of the processor. Thereby, it has fewer transformations as the same as FCS-MPC.

Fig. 2.2 shows a block diagram, where a three-phase VSC with *LC* is included and it is grid-connected[1]. Classical control takes the necessary control actions after an error has occurred. The purpose of the inner current loop is to track the signal from the voltage control loop. Also, it ensures fast dynamic disturbance rejection in the designed bandwidth. Bearing in mind, if the control loop has not prober performance then the overall system performance degrades. Based on that, the current loop is essential as well as the voltage control loop. A simplified block diagram of the closed-loop system is provided in Fig. 2.3. Here $V^*_{c\,\alpha\beta}$ and $i^*_{l\,\alpha\beta}$ are the reference capacitor voltage and current vectors and $i^*_{o\,\alpha\beta}$ is the output current vector. $G_v(s)$ and $G_i(s)$ represent the voltage and current regulators transfer functions (TF), $G_{pwm}(s)$ is the TF related to PWM delays and computation, and $G_{dec}(s)$ is the TF related to the decoupling of the control states. The design approach is considering the cross-coupling between the inductor current and the capacitor voltage. The complete TF for the closed-loop system of the non-ideal decoupling with a unity transfer function is shown in (2.1). Investigations and deep details regarding the decouplings are shown in [21].

$$i_{L\alpha\beta}(s) = \frac{Z(s)C_f^2 s G_i(s) G_{pwm}(s) + G_i(s) G_{pwm}(s) C_f}{Z(s) L_f C_f^2 s^2 + [X]s + [Y]} i^*_{L\alpha\beta}(s) \tag{2.1}$$

[1]Undefined variables in this section can be found in J1 and C3.

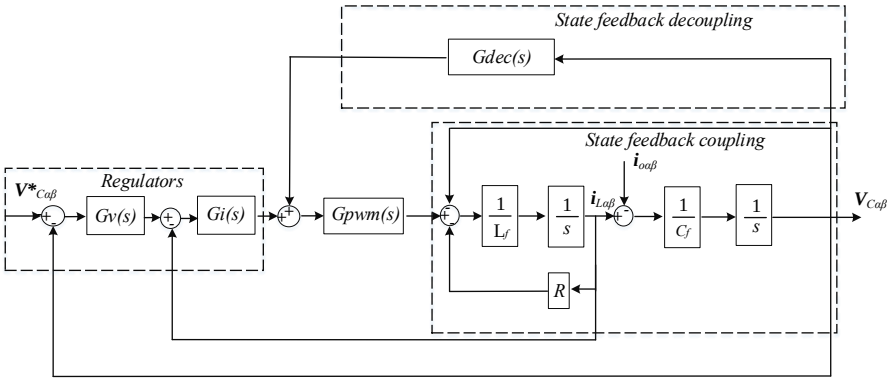

Fig. 2.3: Block diagram of the closed-loop system.

where,

$$X = [Z(s)RC_f^2 + Z(s)C_f^2 G_i(s)G_{pwm}(s) + L_f C_f] \tag{2.2}$$

and,

$$Y = [Z(s)C_f + RC_f + G_i(s)G_{pwm}(s)C_f - Z(s)C_f G_{pwm}(s)] \tag{2.3}$$

This approach has higher damping than without voltage decoupling as mentioned in [21]. In [21], also a complete investigation with respect to the frequency response of such a system has been presented. In that work, the gains of the system are calculated in order to provide a good dynamic response, which is ensured a comparable behaviour between the classical and predictive control as discussed in [C3].

2.2.2 Carrier-based space vector pulse width modulation (CB-SVPWM)

SVPWM control strategy is based on the fact that the possible switching states of VSCs are finite. The typical two-level three-phase VSC has 6 active and 2 zero space (or voltage) vectors. Active vectors produce a nonzero output voltage and zero vectors produce zero output voltage. Space vectors of the three-phase quantities are represented as vectors in a two-dimensional $\alpha\beta$ plan, as shown in Fig. 2.4. So, the concept of SVPWM technique is using the reference voltage vector to identify the sector and calculate the switching time of the pulses. Firstly, it calculates the magnitude and angle of the reference voltage vector. Then the switching time durations of each sector are calculated. Subsequently, the switching signals are calculated in order

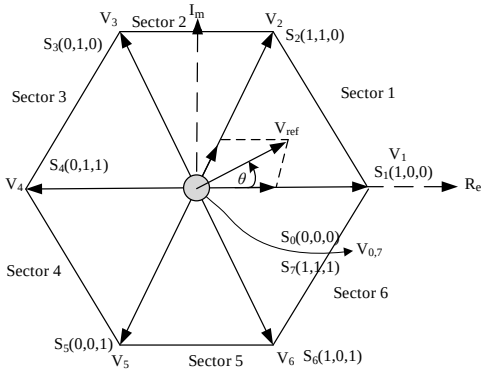

Fig. 2.4: Space vector diagram and the voltage vectors generated by the inverter (V_i).

to compare them with the carrier. This control strategy is implemented in SAPF in this thesis and low distortion of the supply voltage is assumed. As shown in Fig. 2.5, SAPFs generally consist of two distinct main processing, power processing which is accomplished by synthesizing the compensating current that should be drawn from the power system, and signal processing which is determining in real-time the instantaneous compensating current references. The references are passed to the power control stage, which is sending the new actuation to a power converter. The modulation should be at high switching frequency in order to accurately reproduce the compensating current. In this thises, A SAPF is connected to a dc capacitor and

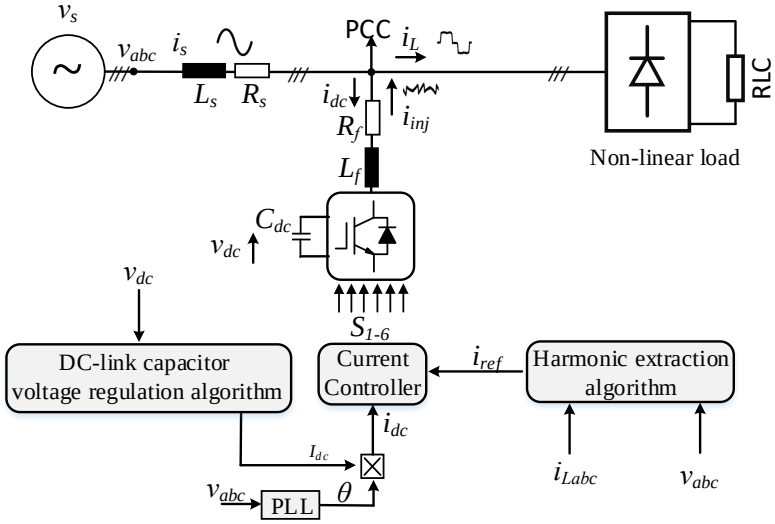

Fig. 2.5: General power circuit and control structure of a shunt active power filter (SAPF).

indicated by the insulated gate bipolar transistors (IGBT)s with antiparallel diode. The active filter controller stage is extracting the harmonics using the dq theory. The new current reference is sent to the current controller which is based on space vector control.

2.3 Model predictive control

Due to the MPC simplicity and easiness to include the constraints and non-linearities of voltage source converter, MPC has been proposed to be applied in many applications such as electrical drives and grid-connected power electronic systems. Specifically, FCS-MPC is based on the principle of using a discrete model of the VSC with an associated filter to predict its future behaviour for all possible control inputs, and consequently, apply the one that minimizes a programmed cost function (CF) at every sampling time [24–26] (see Fig. 2.6). The key idea is to use the raw processing power of the microcontroller to embed all the inner control loops, conventional ac MG structure, within a single algorithm that takes into account the model of the converter and its associated filter. This structure provides flexibility and inherent fast response [27–29]. The model of the system can be obtained in details in [C3 and J1]. Furthermore, in order to reduce the required computational burden, an observer has been used to estimate the load current instead of measuring it. The observer model is explained in details in [C3]. The CF based on one-step prediction horizon becomes problematic when controlling higher-order plants (as is the case of LC filter) due to couplings between different state variables [30, 31]. A solution is proposed, which is explicitly deal with the dynamic coupling between the inductor current and capacitor voltage, allowing the usage of a single-step prediction horizon for effective voltage control of the LC filter in grid-connected applications. In the following, the conventional and the proposed solutions are presented according to the paper [J1 and J2].

2.3.1 Conventional FCS-MPC scheme for voltage regulation

Fig. 2.6 [2] shows a general block diagram of a three-phase VSC based on an FCS-MPC algorithm. In its basic form, the algorithm is executed sequentially, and at the beginning of each sampling time T_s, it applies the new switching configurations, which are calculated based on the previous step. Then, it receives again new and updated measurements in order to select the new switching configurations. The following CF is implemented in a stationary reference frame ($\alpha - \beta$):

$$g = (V^*_{ref_\alpha} - V^p_{c_{f\alpha}}(k+1))^2 + (V^*_{ref_\beta} - V^p_{c_{f\beta}}(k+1))^2 \tag{2.4}$$

[2] Undefined variables in this section can be found in J1.

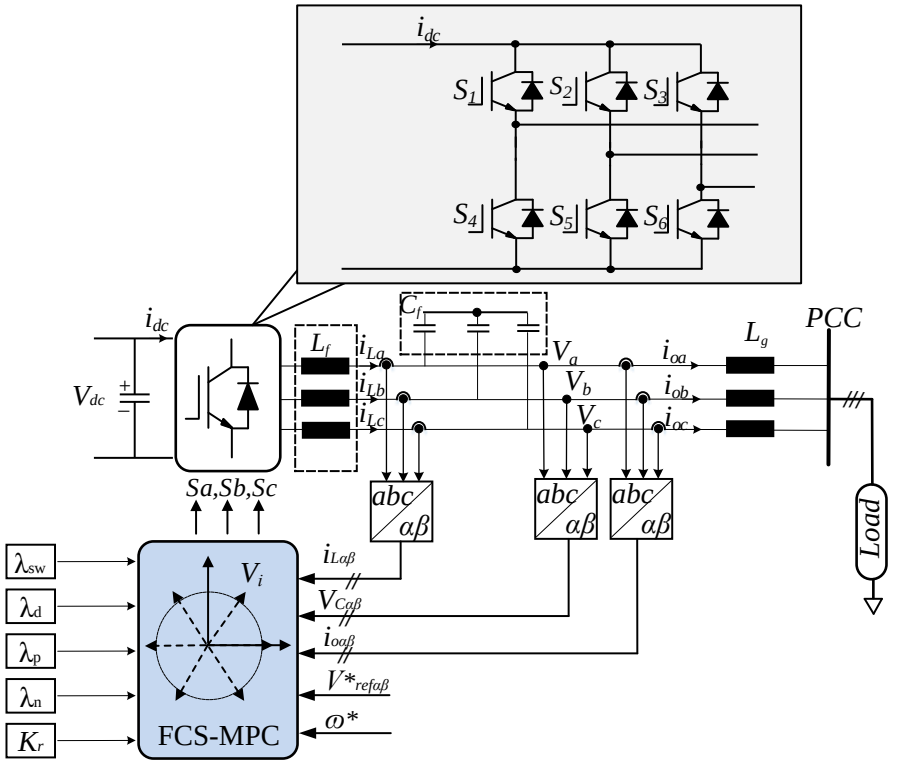

Fig. 2.6: Power circuit and FCS-MPC control structure of the used inverter for microgrid applications.

where g is the CF, $V^*_{ref_\alpha}$ and $V^*_{ref_\beta}$ are the real and imaginary components of voltage reference signals in the stationary reference frame, while $V^p_{c_{f\alpha}}(k+1)$ and $V^p_{c_{f\beta}}(k+1)$ are the predicted components for each possible switching configurations. The conventional tracking method uses a single objective CF, which in this case tracks the voltage and it is directly regulated by the control input. Conventionally, applying a two-step or three-step prediction horizon can improve the power quality. In 2.5, a mathematical CF is shown using two-step prediction. But looking further than one prediction step ahead is optimal only for the first order plants. For second-order plants, capacitor voltage in the *LC* filter configuration is regulated indirectly through the inductor current. By using the conventional tracking method in such configuration, the current cannot change its value instantaneously since the capacitor cannot change its derivative instantaneously. Therefore, no respect is given to the

capacitor voltage derivative, which determines the heading of its trajectory.

$$\begin{aligned} g = (V_{c\alpha}^{*} - V_{c\alpha}^{p}(k+1))^2 + (V_{c\beta}^{*} - V_{c\beta}^{p}(k+1))^2 \\ + (V_{c\alpha}^{*} - V_{c\alpha}^{p}(k+2))^2 + (V_{c\beta}^{*} - V_{c\beta}^{p}(k+2))^2. \end{aligned} \tag{2.5}$$

Thereby, using a multi-step approach to improve the power quality makes the computations too intensive for practical applications. There is another approach by assuming that the same switching configuration will be kept for two periods ahead ($k+2$). This approach requires a highly accurate system model as well as it does not consider the capacitor voltage trajectory during inter-sampling periods [28, 31, 32]. On the other hand, the classical FCS-MPC does not allow control over the switching frequency resulting in low efficiency due to the switching variations. Therefore, there was a need to propose an FCS-MPC scheme where it can overcome these issues.

2.3.2 Proposed FCS-MPC schemes

As discussed above, using the voltage reference as the only objective in grid-connected converters is inadequate specifically with a second-order plant. Also, the absence of switching frequency control causes low efficiency. Therefore, in order to improve the capacitor voltage quality and having a control over the switching frequency compared to the classical strategy, a proposed FCS-MPC scheme is discussed here. The inability to control the derivative of the capacitor voltage is a fundamental cause of high THDv [33]. Therefore, the ideal regulator should track both the voltage reference and its derivative, which can be included as two signals treated as two separate references as follows:

$$\mathbf{v_{c_f}^{*}(t)} = V_{ref} sin(\omega_{ref} t) + j V_{ref} cos(\omega_{ref} t) \tag{2.6}$$

where ω_{ref} and V_{ref} are the frequency and amplitude of the reference signal, respectively. The voltage derivative reference is obtained as follows:

$$\frac{\mathbf{dv_{c_f}^{*}(t)}}{\mathbf{dt}} = \omega_{ref} V_{ref} cos(\omega_{ref} t) - j\omega_{ref} V_{ref} sin(\omega_{ref} t) \tag{2.7}$$

Tracking of $V_{c_f}^{*}(t)$ is already accomplished by the presented CF in (2.4). Now it is needed to design a CF, which will ensure that $\frac{\mathbf{dv_c(t)}}{\mathbf{dt}}$ tracks $\frac{\mathbf{dv_c^{*}(t)}}{\mathbf{dt}}$. In order to ensure that, the predicted value is needed and it can be taken from the predicted currents that are calculated directly from the discrete model of the converter:

$$\frac{\mathbf{dv_{c_f}(t)}}{\mathbf{dt}} = \frac{i_{L\alpha}(t) - i_{o\alpha}(t)}{C_f} + j\frac{i_{L\beta}(t) - i_{o\beta}(t)}{C_f} \tag{2.8}$$

It can be seen that the voltage derivative trajectory will be well tracked if the respective differences between the first and second terms from (2.7) and (2.8)

are minimized. These equations are explicitly formulated in the following CF:

$$\begin{aligned} g_I = &(I_{f\alpha}(k+1) - I_{o\alpha}(k) + C_f\omega_{ref}(V^*_{ref\beta}(k)))^2 \\ &+ (I_{f\beta}(k+1) - I_{o\beta}(k) + C_f\omega_{ref}(V^*_{ref\alpha}(k)))^2 \end{aligned} \tag{2.9}$$

The term g_I can now be added to the conventional CF as in (2.10), and the weight λ_d controls its effect:

$$\begin{aligned} g = &(V^*_{ref_\alpha} - V^p_{c_{f\alpha}}(k+1))^2 + (V^*_{ref_\beta} - V^p_{c_{f\beta}}(k+1))^2 \\ &+ (\lambda_d g_I) \end{aligned} \tag{2.10}$$

Furthermore, as the FCS-MPC controller can accept several objectives in its CF, another objective can be included in order to control the switching frequency. Therefore, a switching frequency control scheme based on periodic algorithm has been included and its importance has been controlled by λ_p. A mathematical CF is shown in (2.11) to illustrate the regulated objectives. Worth to mention that the periodic control algorithm can be regulated by the control input K_r, which indicates to the reference frequency.

$$g = g + \lambda_p g_p + \lambda_d g_I \tag{2.11}$$

In addition, several switching frequency controllers can be added, such as Notch and Simple penalization to the improved CF. Their importance can be controlled by λ_{sw} and λ_n. In the next chapter, the performance of the improved FCS-MPC combined with the switching frequency controllers will be presented and discussed compared to the conventional FCS-MPC.

Finally, a predictive current control has been proposed for controlling the shunt active power filter. The new control structure of SAPF is based on FCS-MPC and it controls the SAPF in order to compensate for the harmonics and unbalanced voltages. In the proposed control structure, the predictive algorithm is using a single objective cost function in order to predict the filter currents to evaluate the error and avoid a tuning process as follows:

$$g = (i^*_{f\alpha} - i^p_{f\alpha}(k+1))^2 + (i^*_{f\beta} - i^p_{f\beta}(k+1))^2. \tag{2.12}$$

Where $i^*_{f\alpha\beta}$ are the reference currents and $i^p_{f\alpha\beta}(k+1)$ are the predicted currents. The algorithm will be intensively discussed in Chapter 4 and a set of simulation and experimental results will be provided.

2.4 Summary

In this chapter, different control strategies of a VSC have been discussed. For grid-forming converters, a CB-PWM control strategy has been presented to

capture the power and this is achieved by implementing a voltage and current control loop in a cascaded structure. A similar control strategy can be applied to improve the power quality, where the SVPWM based control is introduced for the shunt active power filters (SAPFs). On the other hand, several control solutions to realize and achieve similar performance and faster response using the same circuit topology based on FCS-MPC have been also discussed and proposed. For grid forming converters, the first control strategy utilizes the conventional cost function, where the voltage is the controlled objective and there is no weighting factor nither switching frequency control. An alternative and also a proposed solution to control both the voltage and its derivative has also been discussed and proposed, where the cost function of this controller has two objectives and they are controlled by the weighting factor. Moreover, in order to have a fixed switching frequency, another objective can be regulated by a switching frequency reference as a control input. Furthermore, other control objectives can control the switching frequency and they are based on notch filer and simple penalization techniques. For a SAPF, a control structure based on a single objective cost function using FCS-MPC is briefly introduced. The performance of the proposed control strategies compared to the conventional control strategies is provided by both experimental and simulation results in Chapter 4.

Chapter 3

Voltage Source Converter Performance Analysis and Enhancement

MPC can provide a faster transient response, more robustness to parameters variation and inherent stability in a wide range of operating modes compared to the classical control techniques [34–39]. In order to verify this hypothesis, simulation and experiments are carried out using a three-phase grid-connected and stand-alone VSC. In an attempt to gain an initial understanding of the principle operation of the MPC with a VSC, the following traits are discussed and investigated in this chapter:

- Calculation of the predicted variables of the converter using a discrete model of the system. In [C3] the system and also observer models are provided. Worth to mention that the observer model is implemented in some parts of this work to reduce the computational burden by estimating the load current.
- Using the new cost function to improve the overall efficiency of the converter and enhance the power quality too. Also, controlling the switching frequency in order to have a fixed behaviour.
- Validate the performance of the FCS-MPC using a modulator.
- Performance investigation of a VSC in terms of THD, losses, and dynamic response for the introduced and classical cost functions.

3.1 Frequency control

Generally, FCS-MPC without frequency control has a problem of variable switching frequency [25, 26, 40, 41]. That provides difficulties in the *LC* filter design as well as it might reduce the efficiency because of the higher losses. Therefore, much research has been devoted to finding a feasible solution to obtain a fixed switching operation using FCS-MPC [42–45]. In this section, the switching frequency of the proposed CF has been controlled with several methods, as it is illustrated in Fig. 3.1, and their performances will be discussed. The optimal states, which are decided by the MPC control unit

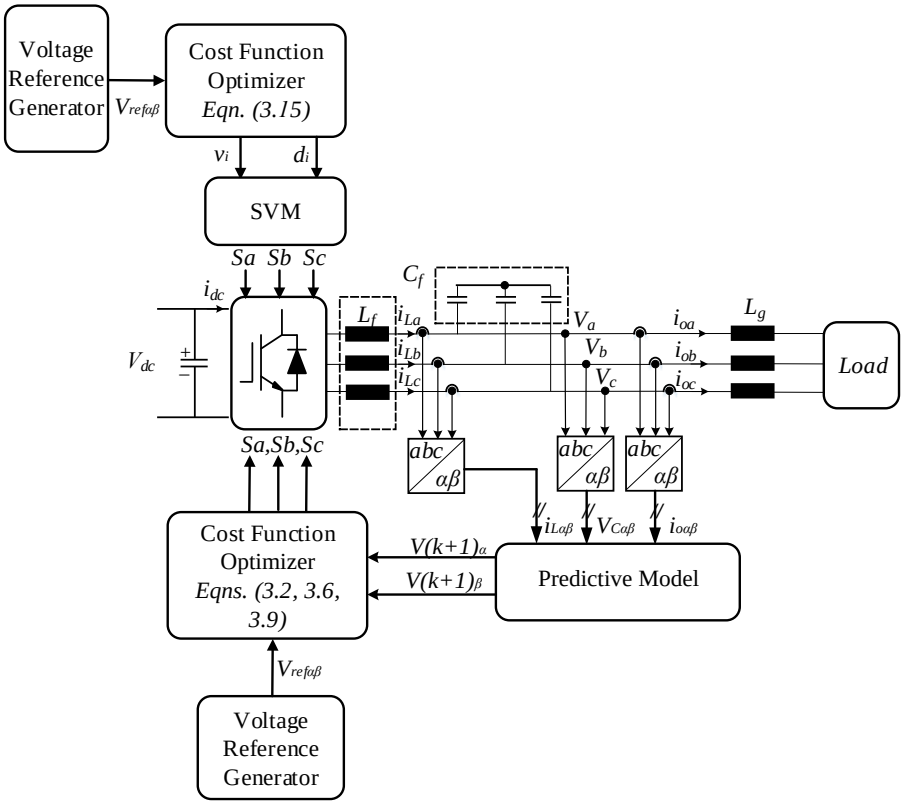

Fig. 3.1: Block diagram showing the different utilized FCS-MPC schemes applied in this study.

to minimize the voltage error, give a random commutation as there is no control over the switching frequency and a considerable amount of losses are introduced. Furthermore, this issue is a fundamental cause of electromagnetic interference, resonances in the system, and unbalanced stresses on the switches. In order to have control over the switching frequency, the CF

should also comply with some requirements such as accurate reference tracking, low computation time, flexibility, and simplicity. Moreover, the included objectives should be evaluated for the minimal error without hindering each other. It is essential to have controllable objectives by including weighting factors in order to achieve the desired power quality or other targets. Thus, the CF should control the switching frequency but not at the expense of the other objectives or with a minimum impact. If one control objective overwhelms another objective, then the control unit will only care about minimizing the considered objective by fading the other objectives or making them less important. In this chapter, the following switching frequency controllers will be applied to the conventional and improved FCS-MPC schemes.

- ☐ Simple Penalization
- ☐ Notch Filter
- ☐ Periodic Control
- ☐ Modulated Model Predictive Control (M^2PC)

As mentioned above, an FCS-MPC scheme based on SVM will also be discussed in order to evaluate the performance of the FCS-MPC schemes compared to a modulated scheme. For the following Subsections, Table 3.1 is describing the parameter values of the considered system in order to perform the experimental and simulation results.

Table 3.1: The filter parameters and sampling times used in simulation and experimental setup.

Parameter	5.5 kVA system (Experimental)	System Model (Simulation)
S	5.5 kVA	5.5 kVA
V_a	230	230
V_{dc}	600	600
ΔI	10%	10%
Q_c	$< 5\%S$	$< 5\%S$
f_g	50 Hz	50 Hz
Z_{Rd}	$X_{Cf}(\omega_r)$	$X_{Cf}(\omega_r)$
f_{res}	$10f_s < f_r < 1/2f_s$	$10f_s < f_r < 1/2f_s$
f_s	40 kHz	*40 kHz in order to compare with the experiments *80 kHz in order to show the sampling effects
L_f	5 mH	*For 80 kHz = 2.5 mH *For 40 kHz = 5 mH
C_f	60 μF	*For 80 kHz = 20 μF *For 40 kHz = 60 μF

3.1.1 Simple penalization

A basic strategy for the switching frequency regulation is through penalizing the act of commutation. The objective can be controlled by the weight λ_{sw} and given as:

$$\Delta S_k = \lambda_{sw}(S_k - S_{k-1})^2. \tag{3.1}$$

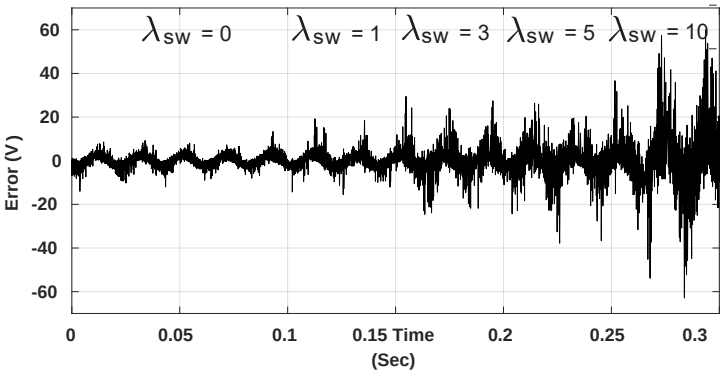

Fig. 3.2: Instantaneous voltage error during the utilization of different weighting factors λ_{sw}.

Usually, the conventional tracking method in the grid forming converter is combined with a simple penalization if a partial control over the switching frequency is needed, and that is known as SP-MPC. In the improved controller, the evaluation of the voltage derivative error is an extra objective to improve the damping ability of the controller. That is known as the SP-IMPC and both cost functions can be shown in (3.2). In the SP-IMPC, if the voltage or its derivative has a large error, then its corresponding value in the cost function would be large enough to overcome the penalization during the switching. Therefore, strong importance should be given to the penalization term in order to maintain the commutation of the last step and to result in switching reduction. Fig. 3.2 illustrates the degradation in the controller ability when giving much importance to the penalization term. This strategy leads to a lower average frequency and higher voltage error. Considering that the spectrum will still be spread in a wide band range and concentrated more to the lower frequencies, as it is shown in Fig. 3.3. When applying the SP strategy, it can enable an observable control over the switching frequency and the dynamic operation remains to behave very fast during the frequent load changes.

$$g_s = \overbrace{\overbrace{g + \lambda_{sw}(S_k - S_{k-1})^2}^{SP-MPC} + g_I}^{SP-IMPC} \tag{3.2}$$

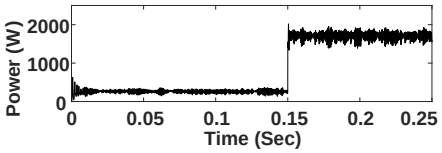

(a) SP-MPC

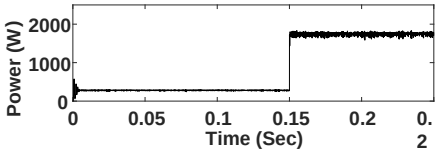

(b) SP-IMPC

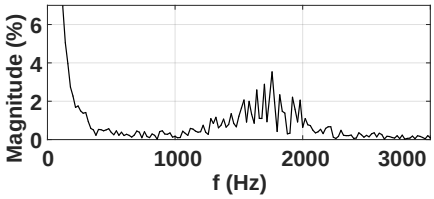

(c) SP-MPC

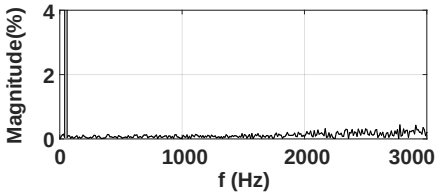

(d) SP-IMPC

Fig. 3.3: Dynamic response of the active power and spectrum shape using a simple penalization frequency control with the conventional and improved MPC. (a) Dynamic response of the active power using SP-MPC ; (b) dynamic response of the active power using SP-IMPC; (c) SP-MPC voltage spectrum; and (d) SP-IMPC voltage spectrum.

3.1.2 Notch filter

Notch filters are shaping the voltage spectrum at different frequencies, where they use different weights in the CF, allowing for harmonics control, as shown in Fig. 3.4. This control approach aims to concentrate the voltage spectrum around the desired frequency utilizing a digital notch filter. The implementation of the notch filter is done in the discrete time domain due to the discrete nature of the MPC. Therefore, the CF can be modified as:

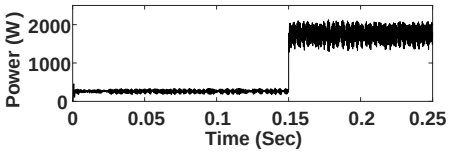

(a) N-MPC

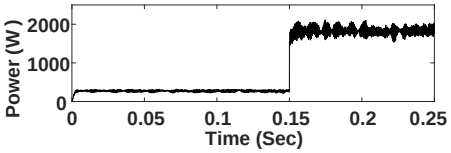

(b) N-IMPC

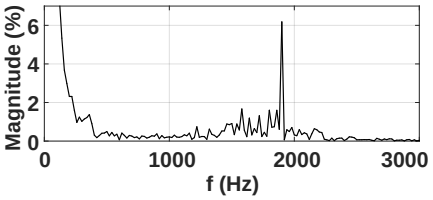

(c) N-MPC

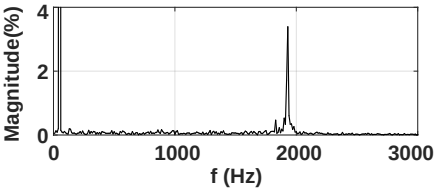

(d) N-IMPC

Fig. 3.4: Dynamic response of the active power and spectrum shape using a notch frequency control with the conventional and improved MPC. (a) Dynamic response of the active power using N-MPC ; (b) dynamic response of the active power using N-IMPC; (c) N-MPC voltage spectrum; and (d) N-IMPC voltage spectrum.

$$g_{m1} = \lambda_n F_n(g) \tag{3.3}$$

where λ_n is the weighting factor and F_n is the second-order band-stop filter. A Tustin discretization of the notch filter is considered in the filter design. Similarly, the derivative term g_I in (2.9) can be modified as:

$$g_{m2} = \lambda_n F_n(g_I) \tag{3.4}$$

The implemented notch filter in this work, which has a frequency concentration at 2 kHz is illustrated in (3.5):[1]

$$\mathbf{H}_{2kH} = \frac{0.9849z^2 - 1.875z + 0.9849}{z^2 - 1.875z + 0.9698} \tag{3.5}$$

In this work, the notch filter is designed for the IMPC scheme, as shown in (3.6) in order to control the switching frequency of the grid-forming converter. Changing the filter bandwidth gives a different concentration range around the desired switching frequency. Finally, weighting factors design for both N-MPC and N-IMPC have been done to obtain the best power quality with minimum switching frequency deviation. In the same manner, the dynamic performance of the FCS-MPC scheme with notch filter is retained. In the low-frequency region, where the concentrated frequency is close to the resonance frequency, the controller fails to achieve a stable operation.

$$g_n = \overbrace{\overbrace{g + \lambda_n F_n (V_{ref} - V_{cf})^2}^{N-MPC} + g_I + \lambda_n F_n (g_I)}^{N-IMPC} \tag{3.6}$$

3.1.3 Periodic control

The key idea of the periodic control strategy is to achieve a modulation behaviour without using a modulator. The periodic control strategy focuses on fixing the time it takes for two consecutive similar commutations as it is shown in [J1]. The objective is to control the T_{up} and T_{down}, as explained in details in [J1]. Moreover, the frequency is compared with a reference time of T_r, which is used for both the up and down switching events in order to achieve the desired performance. Weighting factors design for both P-MPC and P-IMPC have been done to obtain the best power quality with minimum frequency deviation. In that context, Fig. 3.5 shows an example of the proposed tuning method. Also, a flowchart of the periodic control combined with the improved predictive scheme is provided in Fig. 3.6.

The CF in (3.7) is describing the mechanism of the periodic control, elaborating how the up and down switching events can be evaluated and included in the main CF.

$$g_p = \lambda_p((T_{up} - T_r)^2 + (T_{down} - T_r)^2) \tag{3.7}$$

where the CF can be rewritten as the following:

$$g_p = \lambda_p((K_{up} - K_r)^2 T_s^2 + (K_{down} - K_r)^2 T_s^2) \tag{3.8}$$

[1]Switching frequency is concentrated at 2 kHz in order to compare Notch filter performance with the other switching frequency algorithms in J1.

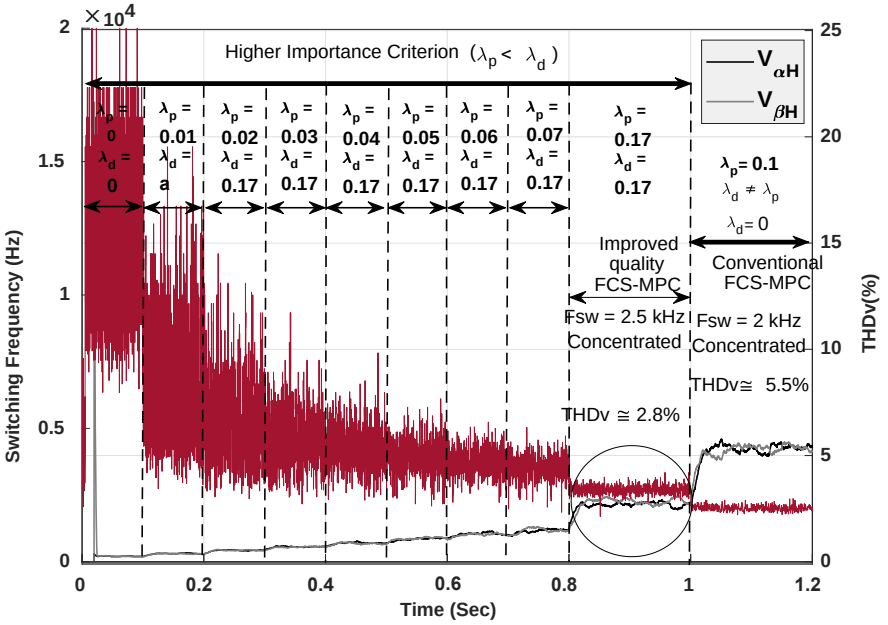

Fig. 3.5: Illustration of importance of weights, where the derivative weighting factor λ_d is higher and equal in importance than the periodic weighting factor λ_p.

The algorithm predicts the state of $K_{up} = \frac{T_{up}}{T_s}$ and $K_{down} = \frac{T_{down}}{T_s}$ for all possible states as menstioned earlier and discussed in [J1]. $K_r = \frac{f_s}{f_r}$ is the reference frequency that is provided to the MPC unit to reshape the spectrum. The factor λ_p is used to mitigate the deviation and objective importance. CFs of the conventional and improved periodic schemes are shown in (3.9). Furthermore, the performance of the algorithm during the dynamic changes and its spectrum are shown in Fig. 3.7. The results indicate that the periodic FCS-MPC scheme has control over the switching frequency, where the output power quality is very high compared to the other control strategies mentioned above. No negative effects on the dynamic performance are observed and that makes P-IMPC feasible and to be considered it in a wide range of applications.

$$g_p = \overbrace{\overbrace{g + \lambda_p((K_{up} - K_r)^2 T_s^2 + (K_{down} - K_r)^2 T_s^2)}^{P-MPC} + g_I}^{P-IMPC} \tag{3.9}$$

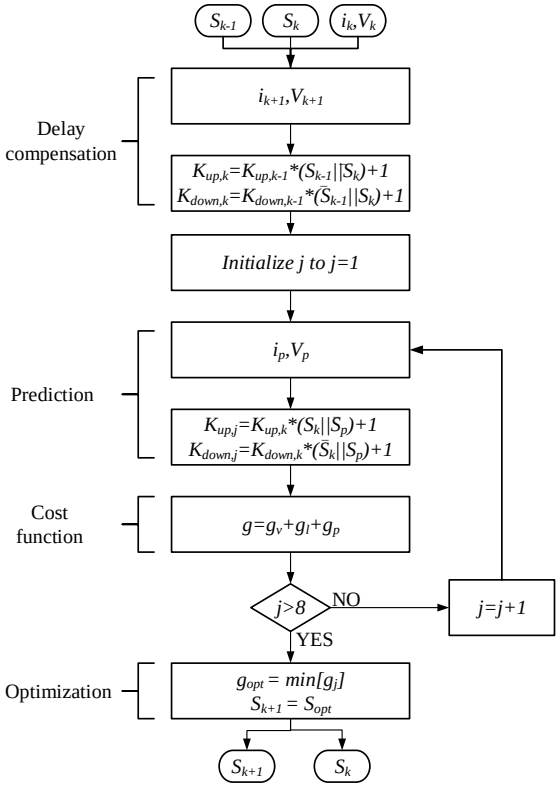

Fig. 3.6: Flowchart showing the implementation of P-IMPC.

3.1.4 Modulated model predictive control (M^{2}PC)

For the 2L-VSC, it is possible to define each available vector using space vector control [25, 26, 40] in $\alpha\beta$ plan as shown in Fig. 3.8. The algorithm calculates the prediction of two active vectors that form each sector at every T_s and evaluates for the pre-programmed cost function. Here, the cost function is defined by (2.4), and it is evaluated for each sector. Each prediction is evaluated based on a model given in [J3]. Duty cycles for the active vectors are calculated by solving the following:

$$d_i = \frac{\delta}{g_{si}} \tag{3.10}$$

where δ is the proportionality constant, the subscript i denotes the adjacent vector, in this case (i = 1; 2) and i = 0 correspond to the duty cycle of a zero vector.

$$d_o + d_1 + d_2 = T_s \tag{3.11}$$

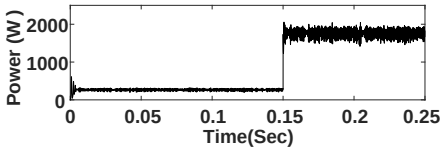

(a) P-MPC

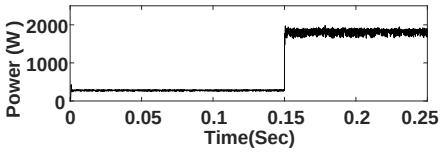

(b) P-IMPC

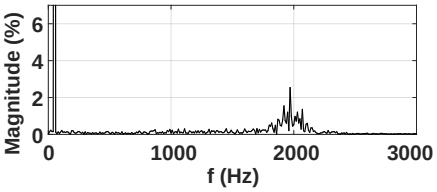

(c) P-MPC

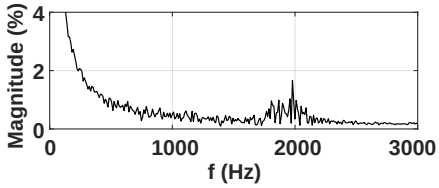

(d) P-IMPC

Fig. 3.7: Dynamic response of the active power and spectrum shape using the periodic frequency control with the conventional and improved MPC. (a) Dynamic response of the active power using P-MPC ; (b) dynamic response of the active power using P-IMPC; (c) P-MPC voltage spectrum; and (d) P-IMPC voltage spectrum shape.

By solving the previous equations (3.10)-(3.11), it is possible to obtain duty cycles for each vector value as given:

$$d_o = \frac{T_s g_1 g_2}{g_o g_1 + g_1 g_2 + g_o g_2} \tag{3.12}$$

$$d_1 = \frac{T_s g_o g_2}{g_o g_1 + g_1 g_2 + g_o g_2} \tag{3.13}$$

$$d_2 = \frac{T_s g_o g_1}{g_o g_1 + g_1 g_2 + g_o g_2} \tag{3.14}$$

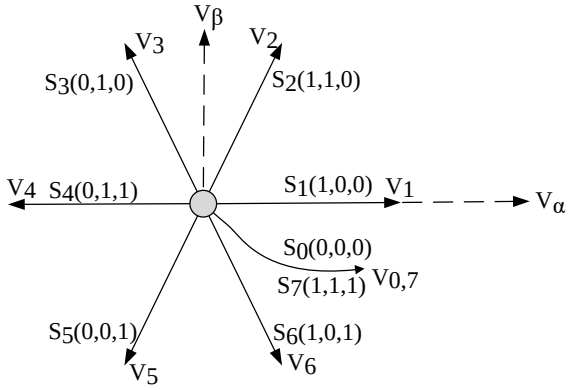

Fig. 3.8: Voltage vectors (V_i) generated by the inverter.

Then a new cost function, which is evaluated at every T_s, is defined as:

$$g(k+1) = d_1 g_1 + d_2 g_2 \tag{3.15}$$

Then, the duty cycles are obtained and the optimal two vectors are selected. Hence, the following equations are defining the active times for each vector:

$$\begin{aligned} T_o &= T_s d_o \\ T_1 &= T_s d_1 \\ T_2 &= T_s d_2 \end{aligned} \tag{3.16}$$

It has been found that the behaviour of the predictive fixed voltage control has degraded the overall performance in the case of low switching frequency operation as it is discussed in [J3]. Fig. 3.9 shows part of the results when applying the modulation strategy. The spectrum analysis shows that higher switchings are needed. But in this case, the switchings at 5 kHz is implemented for the sake of comparison.

3.2 Harmonics evaluation

In this work, an intensive investigation has been done in order to validate the power quality of different FCS-MPC schemes. The investigations can be described into four folds; 1) Evaluation for one-step prediction horizon, 2) Evaluation of multi-step prediction horizon[2], 3) Evaluation for different fixed

[2]For one and multi-step, parameters in Table 3.2 are used.

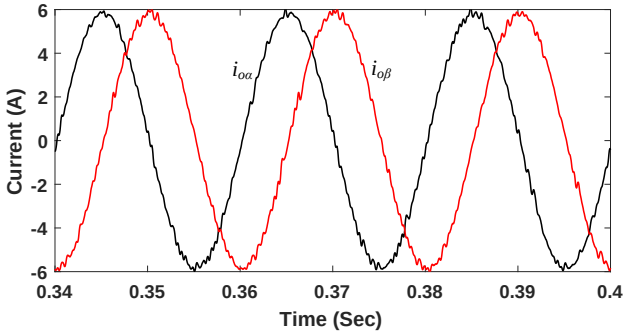

(a)

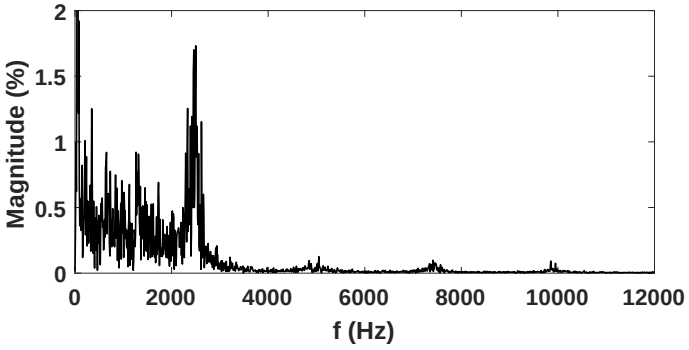

(b)

Fig. 3.9: (a) Obtained $I_{o\alpha\beta}$ currents using M^{2}PC , and (b) obtained voltage spectrum using M^{2}PC

switching frequency FCS-MPC schemes [3], and 4) Extended power quality evaluation for modulated and non-modulated MPC schemes [4].

3.2.1 THDv Evaluation for one-step and multi-step prediction using the conventional CF.

In order to achieve a fair comparison, the parameters, and operating conditions as mentioned in Table 3.2[5] are applied for studied FCS-MPC schemes in this part. The assessment aims to determine the optimum output voltages for grid-forming converters in terms of THDv with the possibility of reduced calculation burden. Hence, the following conventional CFs were applied, and they can be described as:

[3]For fixed switching frequency without a modulator, parameters in Table 3.1 are used.
[4]For fixed switching frequency with a modulator, parameters in Table 3.7 are used.
[5]Compensation indicates to a reduced average switching frequency.

Table 3.2: Parameters of the used three-phase voltage source converter (VSC) in harmonics evaluation.

Quantity	**Value**
DC link voltage V_{dc}	520 V
Filter inductance L_f	2.4 mH
Filter capacitor C_f	25 μF
Resistive load R	50 Ohm
Average switching frequency without compensation	8.3 kHz
Average switching frequency with compensation	5.3 kHz

For one-step prediction:

$$g = (V_{c\alpha}^{*} - V_{c\alpha}^{p})^2 + (V_{c\beta}^{*} - V_{c\beta}^{p})^2 + (\lambda_{sw} n_{sw}^{p}) \tag{3.17}$$

For multi-steps prediction:

$$\begin{aligned} g = {} & (V_{c\alpha}^{*} - V_{c\alpha}^{p}(k+1))^2 + (V_{c\beta}^{*} - V_{c\beta}^{p}(k+1))^2 \\ & + (V_{c\alpha}^{*} - V_{c\alpha}^{p}(k+2))^2 + (V_{c\beta}^{*} - V_{c\beta}^{p}(k+2))^2 + \lambda_{sw} n_{sw}^{p} \end{aligned} \tag{3.18}$$

where $n_{sw}^{p} = (S_k - S_{k-1})^2$. The following Table 3.3 summarizes the achieved results based on the discussed CFs in (3.18). It is worth to notice that the CF contains a switching frequency controller (SP), which is used to address the power quality at different average switching frequencies.

Table 3.3: Comparison of the THDv using different cost functions and considering frequency compensation.

Cost Function (CF)	**THDv**
One step prediction	2.16%
Two Steps prediction	1.27%
Three Steps prediction	1.21%
Four Steps prediction	1.23%
One step prediction with current control	1.20%

3.2.2 THDv Evaluation for one-step and multi-step prediction using the improved CF.

Similarly, the proposed CF objective, which is discussed in details in (2.9), is added to the conventional CF. In line with the evaluation criterion discussed

in the previous subsection, the improved CF has been evaluated following one-step prediction and multi-step prediction methods as the following:

For one-step prediction:

$$\begin{aligned} g = &(V_{c\alpha}^{*} - V_{c\alpha}^{p})^2 + (V_{c\beta}^{*} - V_{c\beta}^{p})^2 + (I_{f\alpha} - I_{o\alpha} + C\omega_{ref}(V_{c\beta}^{*})^2)^2 \\ &+ ((I_{f\beta} - I_{o\beta} + C\omega_{ref}(V_{c\alpha}^{*})^2)^2 \end{aligned} \tag{3.19}$$

For multi-step prediction:

$$\begin{aligned} g = &(V_{c\alpha}^{*} - V_{c\alpha}^{p}(k+1))^2 + (V_{c\beta}^{*} - V_{c\beta}^{p}(k+1))^2 + (V_{c\alpha}^{*} - V_{c\alpha}^{p}(k+2))^2 \\ &+ (V_{c\beta}^{*} - V_{c\beta}^{p}(k+2))^2 + (I_{f\alpha} - I_{o\alpha} + C\omega_{ref}(V_{c\beta}^{*})^2)^2 \\ &+ ((I_{f\beta} - I_{o\beta} + C\omega_{ref}(V_{c\alpha}^{*})^2)^2 \end{aligned} \tag{3.20}$$

Then, the following Table 3.4 summarizes the achieved results based on the discussed CFs in (3.20).

Table 3.4: Comparison of the THDv using different cost functions and not considering frequency compensation.

Cost Function (CF)	**THDv**
One step prediction	1.20%
Two Steps prediction	0.71%
Three Steps prediction	0.69%
Four Steps prediction	0.69%
One step prediction with current control	0.74%

It can be noticed from the output results that no further THDv improvement can be obtained by applying a prediction step more that three-step prediction horizon. Also, the improved CF give high power quality and has low computation. Secondly, a reduction of the average switching frequency results in higher harmonic distortion.

3.2.3 THDv evaluation for different fixed switching frequencies MPC schemes.

Furthermore, using the parameters discussed in Table 3.1, simple penalization, notch filter, periodic control strategies have been evaluated for grid-forming converters in terms of THDv. The following Tables 3.5 and 3.6 summarize the power quality based on the discussed fixed switching frequency schemes. The results demonstrate the power quality in case of using the conventional and the improved scheme.

Table 3.5: THDv and current error for the used frequency control methods in this study at 2 kHz, 1 kW

Control method	THDv	Current error
Simple penalization (SP-MPC)	7.52%	3.90%
Notch filter (N-MPC)	5.67%	2.23%
Periodic control (P-MPC)	5.51%	2.62%

Table 3.6: THDv and current error for the used frequency control methods in this study using the improved CF at 2 kHz, 1 kW.

Control method	THDv	Current error
Simple penalization (SP-IMPC)	2.62%	1.35%
Notch filter (N-IMPC)	4.14%	1.51%
Periodic control (P-IMPC)	3.11%	0.23%

3.2.4 Extended power quality evaluation for modulated and non-modulated MPC schemes.

In another comparison, the THDv for the Conventional MPC, Improved MPC, Periodic MPC, and Modulated MPC are shown in this part using the parameters in given Table 3.7. Fig. 3.10, it summarizes the obtained THDv results up to 8 kW power rating.

Table 3.7: System parameters used for the simulation and experiments setup using M^2PC.

Parameter	Quantity
S	15 kVA
V_{oa}	230 V(rms)
V_{dc}	600 V
f_g	50 Hz
f_{swav}	$\approx$ 5 kHz
L_f	3 mH
C_f	40 μF

It can be seen that the prediction in one-step or even multi-step horizon is a remarkable feature of the predictive control. Multi-step prediction can mitigate the harmonic content, but it needs a higher amount of calculations.

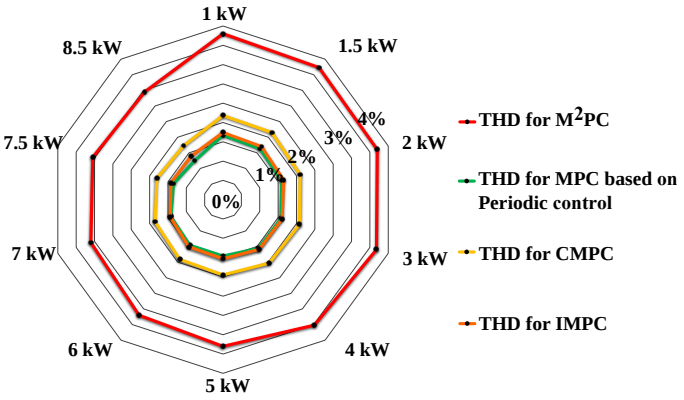

Fig. 3.10: THDv of different modulated and non-modulated MPC schemes at 5 kHz switching frequency (Average).

This issue can be solved by using the improved CF, which is discussed in (2.9). It provides an improvement of the controller damping ability. Furthermore, it reduces the calculation burden of the controller. On the other hand, the power quality of different fixed switching frequencies FCS-MPC schemes has been evaluated. The proposed FCS-MPC scheme and combined with the periodic control showed an improvement in terms of THDv and also excellent fixed switching behaviour. Finally, a comparison has been made for the periodic control, which is not using a modulator, with a modulated MPC, where it is based on space vector control and embedded with a modulator. At lower switching frequency concentrations, the periodic control showed superiority in terms of power quality. Therefore, the periodic control combined with the IMPC has a better ability to have control over the switching frequency, while it retains all the FCS-MPC features. Also, a modulator is not needed, which introduces more simplicity to the configuration.

3.3 Losses evaluation

Power loss is the main issue, which causes efficiency reduction and heat generation. The heat in semiconductor devices should never be higher than a certain junction temperature (Tj) [46–49]. The junction temperature allowed in a switching device module is usually up to 125 °C. In order to study the losses in any power converter, a PLECS toolbox is used for developing the thermal model of the power converter and it is used to calculate both conduction and switching loss.

In PLECS, thermal resistance exists due to the internal construction of the power module. Firstly, the thermal resistance must be as small as possible. Secondly, heat must be transferred from the conducting device into the heat

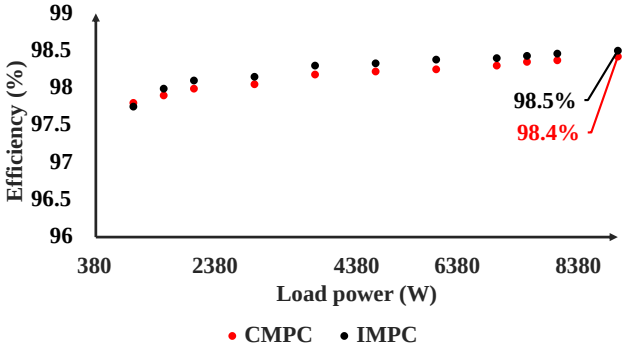

Fig. 3.11: Measured efficiency of the three-phase VSC based on the variable switching frequency schemes, and feeding a linear load.

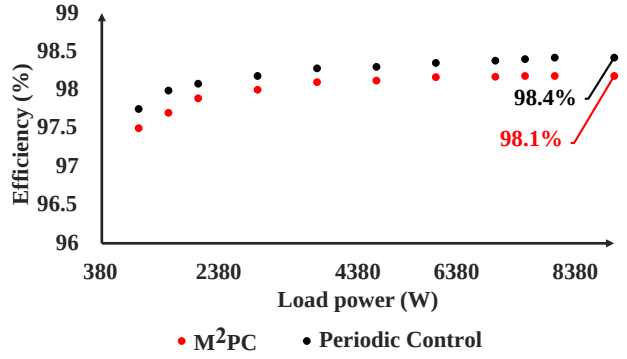

Fig. 3.12: Measured efficiency of the three-phase VSC based on the fixed switching frequency schemes, and feeding a linear load.

sink. In PLECS, the heat sink is modelled, where all equivalent thermal resistances are added and an ambient temperature of 40 °C is considered. Practically, the power analyzer KinetiQ PPA5530 has been used to calculate the power loss.

In the following, Figs. 3.11 and 3.12 show the measured efficiency up to 8 kW using MPC algorithms, which can be found in [J3]. A similar discussion was presented in [C3, C4] between the conventional and the improved FCS-MPC schemes for lower power. Furthermore, the losses distributions were discussed in the same papers [J3 and C4], as shown in Fig. 3.13. In papers [C3, C4], the efficiency of the improved FCS-MPC, conventional FCS-MPC, and CB-PWM was discussed for linear and non-linear loads as also shown in Figs. 3.14 and 3.15. It can be seen that the efficiency of predictive control is getting improved using the improved FCS-MPC scheme. The conventional FCS-MPC scheme has higher losses due to its inability to regulate the output

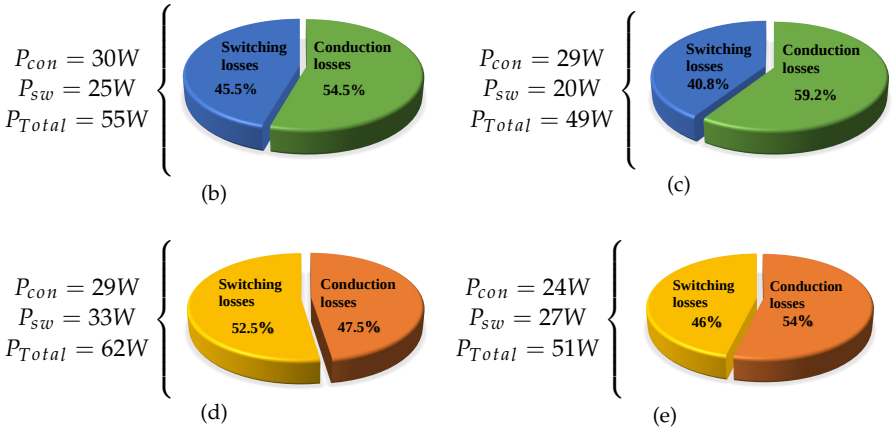

Fig. 3.13: Efficiency assessment at 4 kW rated power using the different FCS-MPC schemes. (b) Distribution of switching and conduction losses for the VSC using the conventional (CMPC); (c) distribution of switching and conduction losses for the VSC using the improved (IMPC) scheme; (d) distribution of switching and conduction losses for the VSC using the (M^2PC) scheme; and (e) distribution of switching and conduction losses for the VSC using the periodic (PMPC) scheme.

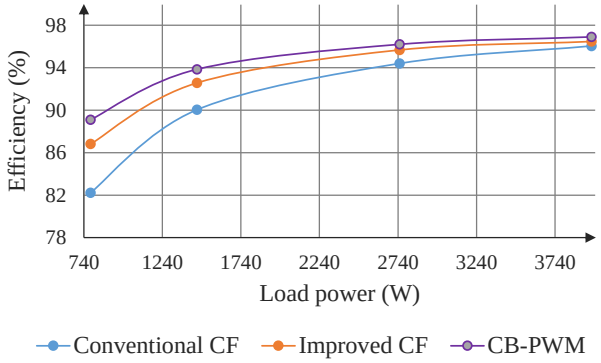

Fig. 3.14: Measured efficiency of the three-phase VSC using conventional FCS-MPC, improved FCS-MPC, and classical carrier-based controllers, for feeding a linear load.

voltage effectively. Moreover, high switching frequency variation, including the upper limit up to the Nyquist frequency, is providing a lower efficiency. The periodic control, combined with the conventional and improved FCS-MPC gives an improvement in term of efficiency. The reason is that the periodic control provides tighter limits and bands reduction of the switching variation.

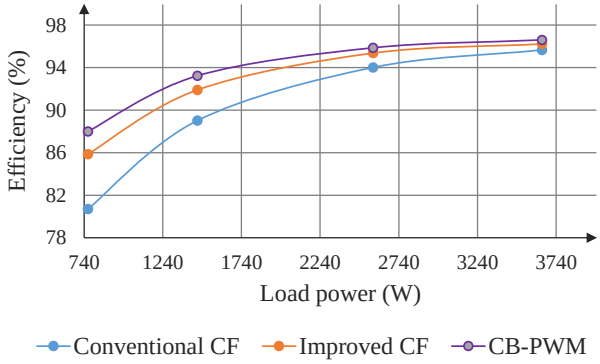

Fig. 3.15: Measured efficiency of the three-phase VSC using conventional FCS-MPC, improved FCS-MPC, and classical carrier-based controllers, for feeding a non-linear load.

3.4 Transient operation

Transient performance of the predictive algorithms have been tested and also compared to the classical algorithms. A load step change has been used to examine the behaviour of the transient reaction of controllers during the transient operations. Fig. 3.16 shows how the improved predictive controller behaves during the load variation and the voltage deviation. Compared to the behaviour in [50], it can be clearly seen that the dynamic response of the general MPC approach is approximately ten times faster rather than the classical methods, which have hierarchical loops to control the power.

On the other side, Fig. 3.17 shows that no significant effect on FCS-MPC characteristics when using frequency control algorithms. It can be seen easily that the dynamic response using the SP-IMPC, N-IMPC, and P-IMPC is maintained. Moreover, P-IMPC has around 5% reduction in the power fluctuation compared to the P-MPC, which is an excellent outcome compared to the N-IMPC and SP-IMPC. It can be concluded that the dynamic response of the FCS-MPC is not affected due to the inherent fast restoration provided by the FCS-MPC control unit.

3.5 Robustness to the parameter mismatch

The robustness of the predictive control algorithm to model parameter variation is also investigated. The behaviour of the system is tested using classical control, which has been done in many research works [19, 21, 50–53]. In order to test the robustness, different combinations of L and C are applied. As shown in Table 3.8, the considered combinations give a clear picture of the robustness of the FCS-MPC controller during the line impedance changes. The combination is considered up to 50% variation in the L and C. It can

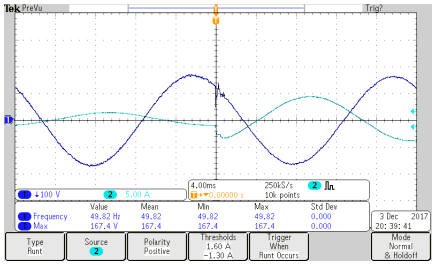

(a)

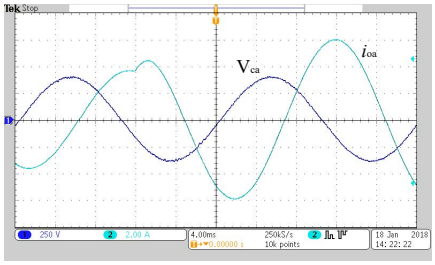
V_{ca}
I_{oa}

(b)

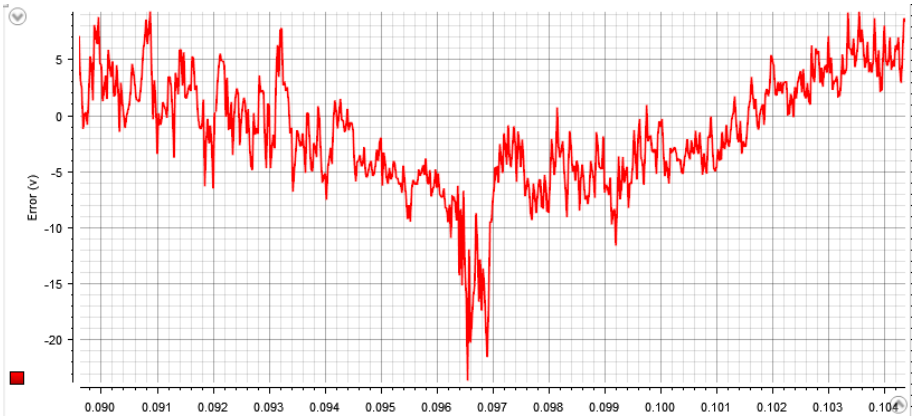
Error (v)
5
0
-5
-10
-15
-20
0.090
0.091
0.092
0.093
0.094
0.095
0.096
0.097
0.098
0.099
0.100
0.101
0.102
0.103
0.104

(c)

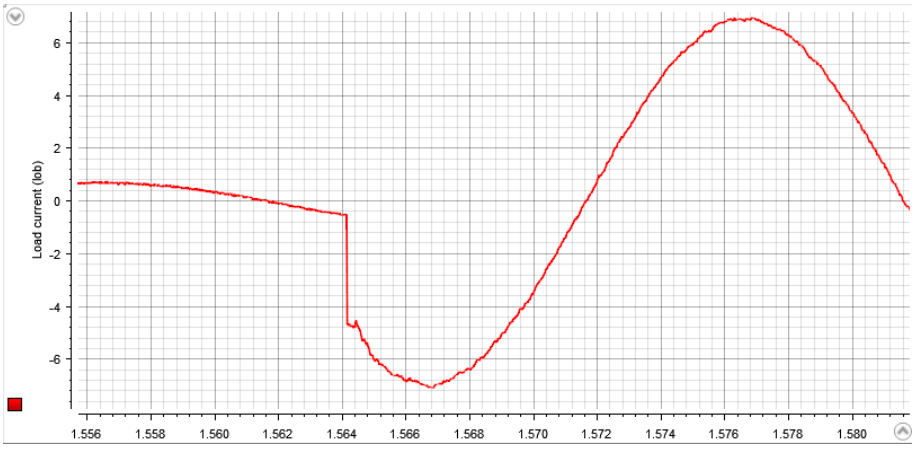
Load current (Iob)
6
4
2
0
-2
-4
-6
1.556
1.558
1.560
1.562
1.564
1.566
1.568
1.570
1.572
1.574
1.576
1.578
1.580

(d)

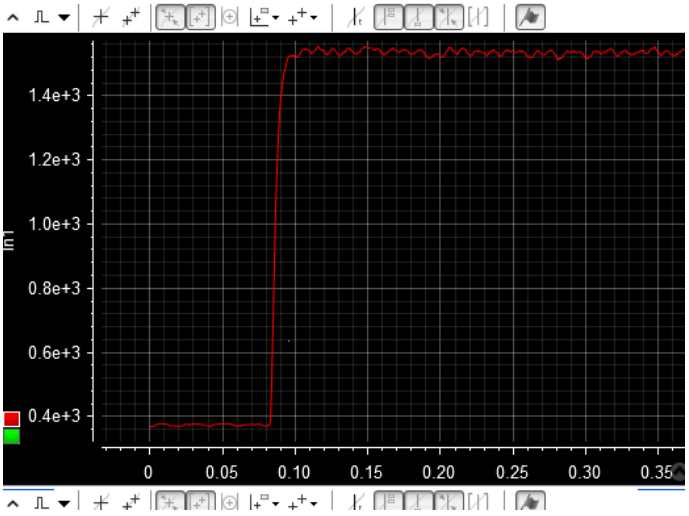

(e)

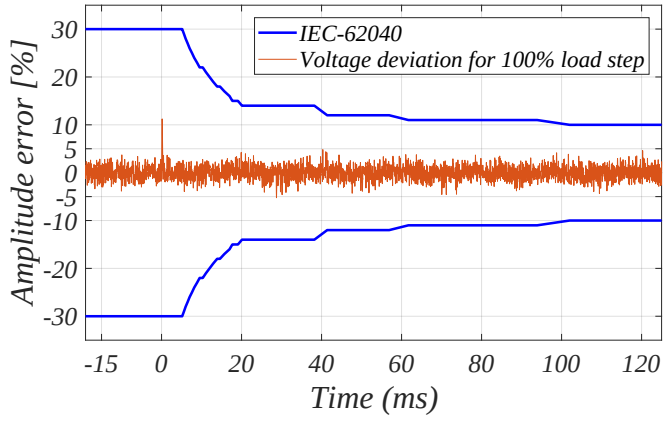

(f)

Fig. 3.16: Transient response of a three-phase VSC using FCS-MPC algorithm. (a) Current behaviour of a load step change, feeding an R load; (b) current behaviour of a load step change, feeding an RL load; (c) voltage error at the transient moment, feeding an R load; (d) current behaviour of a load step change, feeding lower R load (higher power); (e) active power during the transient operation, feeding an R load; and (f) voltage deviation at the transient moment, feeding an R load and following IEC-62040 standard.

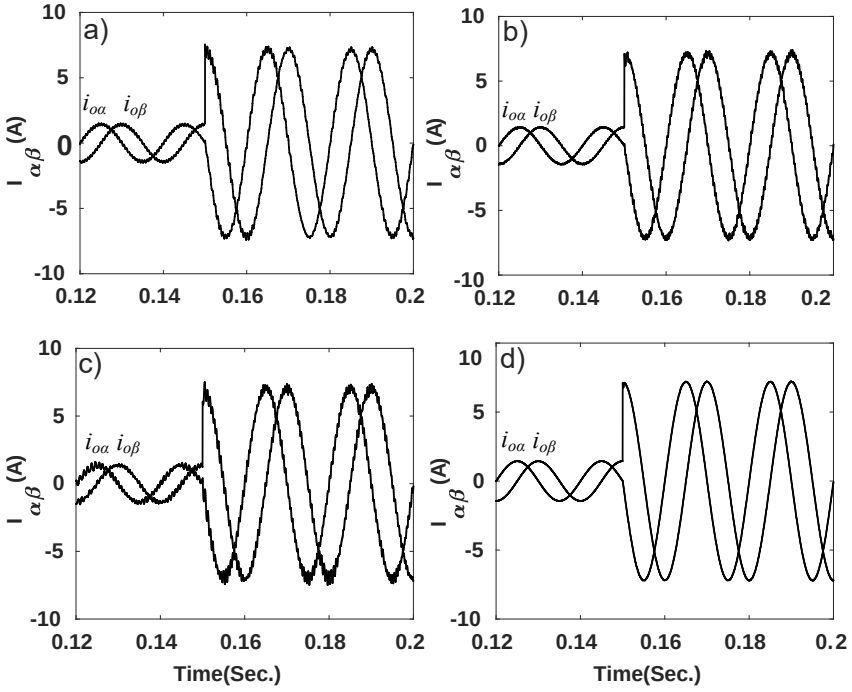

Fig. 3.17: Obtained experimental results showing the dynamic response of the three-phase VSC using the proposed frequency control CFs; load step from 270 W to 1880 W; where (a) is the dynamic response of the N-IMPC strategy; (b) periodic (P-IMPC); (c) simple penalization (SP-IMPC); and (d) no frequency control.

be noticed that improved FCS-MPC is very robust even though in a severe change of L and C, and its stability has been preserved. In Fig. 3.18 different tests have been carried out and presented. Mostly, improved FCS-MPC is not sensitive to parameter variations compared to the conventional FCS-MPC scheme. For instance, in Fig. 3.18(c) conventional FCS-MPC has responded badly when the physical L does not match the considered inductance in the system model.

3.6 Grid-connected inverter based on FCS-MPC

The resonance interaction between the filter inductors and capacitors is the main reason behind the problems that arise with LCL filters associated with 2L-VSC. One remedy for this problem is to propose a solution where the dynamics of the LCL filter are naturally decoupled by the FCS-MPC, which can generate the voltage reference on the filter capacitor. By designing this control unit and considering the bandwidth, the VSC and the LC part of

Table 3.8: Different combinations of L and C to study the robustness of the conventional and improved FCS-MPC schemes

Filter inductance	Filter capacitance	Figure	Current
L_f= 1.2 mH	C_f= 25μF	Fig. 3.18(a)	$I_{o\alpha\beta}$ =1.5 A
L_f= 2.4 mH	C_f= 12.5μF	Fig. 3.18(b)	$I_{o\alpha\beta}$ =1.5 A
L_f= 4.8 mH	C_f= 25μF	Fig. 3.18(c)	$I_{o\alpha\beta}$ =1.5 A
L_f= 4.8 mH	C_f= 25μF	Fig. 3.18(d)	$I_{o\alpha\beta}$ =1.5 A
L_f= 2.4 mH	C_f= 50μF	Fig. 3.18(e)	$I_{o\alpha\beta}$ =1.5 A
L_f= 2.4 mH	C_f= 50μF	Fig. 3.18(f)	$I_{o\alpha\beta}$ =1.5 A
L_f= 4.8 mH	C_f= 50μF	Fig. 3.18(g)	$I_{o\alpha\beta}$ =1.5 A
L_f= 1.2 mH	C_f= 12.5μF	Fig. 3.18(h)	$I_{o\alpha\beta}$ =1.5 A

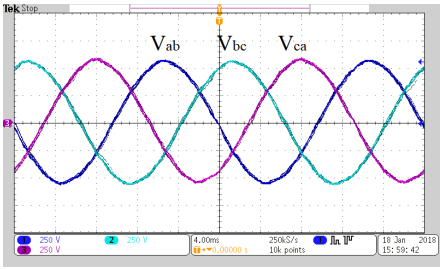

(a)

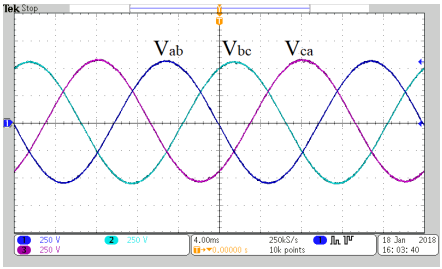

(b)

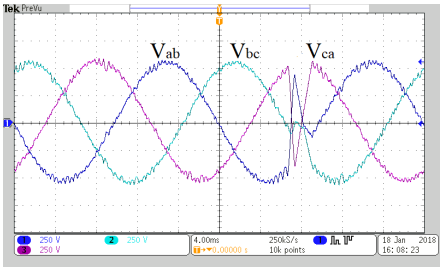

(c)

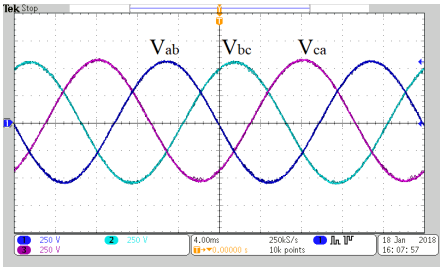

(d)

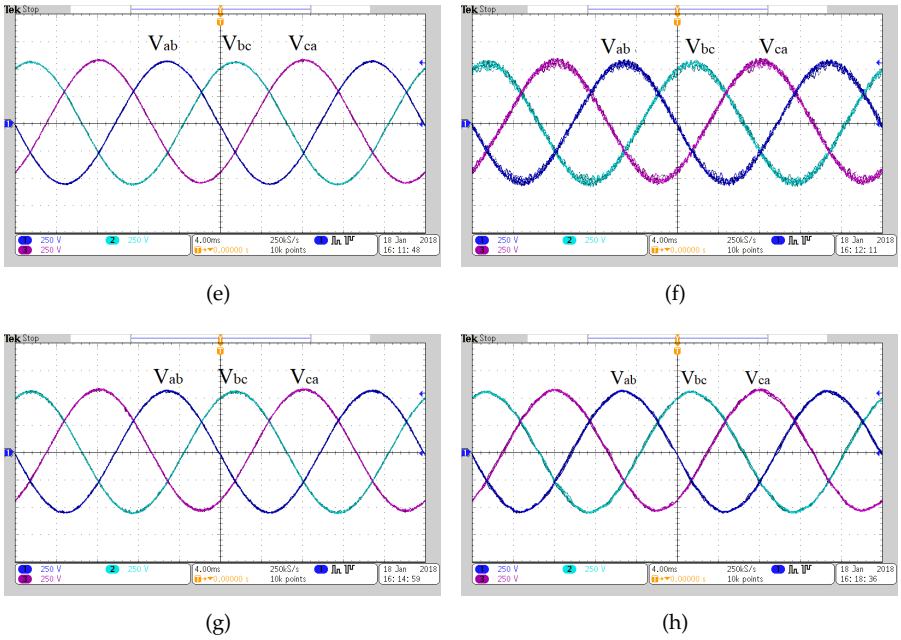

Fig. 3.18: Parameter mismatch test for a three-phase VSC using FCS-MPC algorithm for different L_f and C_f settings. (a) L_f = 1.2 mH and C_f = 25 uF at a load current = 1.5 Amps using improved FCS-MPC; (b) L_f = 2.4 mH and C_f = 12.5 uF at a load current = 1.5 Amps using improved FCS-MPC; (c) L_f = 4.8 mH and C_f = 25 uF at a load current = 1.5 Amps using conventional FCS-MPC; (d) L_f = 4.8 mH and C_f = 25 uF at a load current = 1.5 Amps using improved FCS-MPC; (e) L_f = 4.8 mH and C_f = 25 uF at a load current = 1.5 Amps using improved FCS-MPC; (f) L_f = 2.4 mH and C_f = 50 uF at a load current = 1.5 Amps using improved FCS-MPC; (g) L_f = 2.4 mH and C_f = 50 uF at a load current = 1.5 Amps using conventional FCS-MPC; and (h) L_f = 4.8 mH and C_f = 50 uF at a load current = 1.5 Amps using improved FCS-MPC.

the filter can be treated as an ideal controlled voltage source. Hence, a proportional resonant (PR) controller in $\alpha\beta$ frame can control a plant consisting of the grid-side filter inductor and grid impedance. In that way, the feasibility of this method is greatly enhanced by the improved FCS-MPC scheme, which has been discussed earlier. This method has the benefit of reducing the output voltage harmonic distortion. The voltage reference, provided by the PR controllers, is actuated by the improved FCS-MPC algorithm to select the switching states that minimise the predefined cost function at every sampling instance. Figs 3.19 illustrate how the variable switching frequency method replaces the fixed switching frequency method (PWM). Fig. 3.20 demonstrates the performance of the proposed control structure for grid-connected VSC regulated by IMPC.

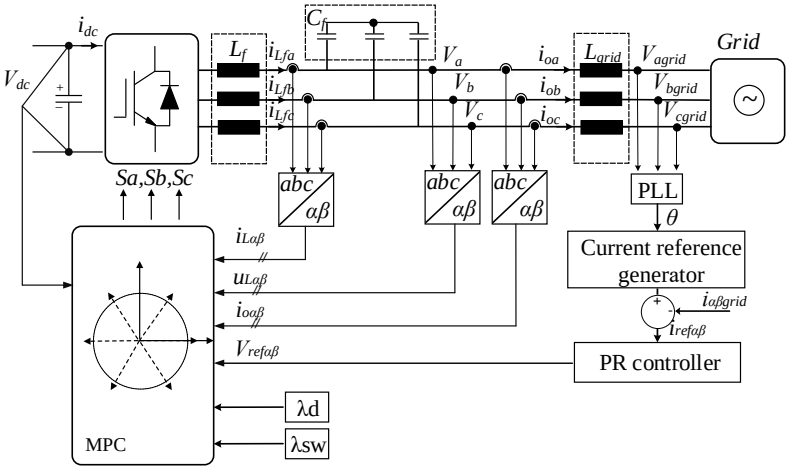

Fig. 3.19: Control structure of the grid-connected VSC based on FCS-MPC.

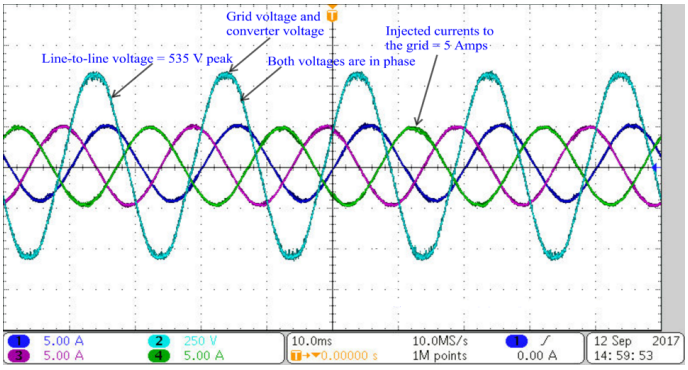

Fig. 3.20: Measured grid voltage and currents of the grid-connected VSC based on improved FCS-MPC. The achieved sampling time (T_s) is equal to 25 μS while the filter inductance and filter capacitance are equal to 2.4 mH and 15 μF, respectively. The grid inductance was equal to 3 mH.

3.7 Summary

In this chapter, the overall performance of the power electronic converter using different FCS-MPC schemes is studied considering many aspects such as power quality, prediction horizon, power losses, efficiency, dynamic changes, and parameters mismatch. For the stand-alone applications and using MPC, the operation and performance of the inverter are not highly dependent on the line impedance characteristics, which are considered as a source of uncertainties in the performance evaluation. From the dynamic response point of view, MPC has a very fast restoration mechanism compared to classical control methods. The results have shown that the performance of the VSC in the steady-state operation can be improved by using different FCS-MPC schemes. Specifically, the MPC scheme where the voltage and its derivative are tracked simultaneously and that introduces higher power quality. Finally, some investigation regarding the grid-connected inverter using the improved FCS-MPC has been shown and explained. In conclusion, simulations and experimental tests were employed to demonstrate the performance of different controllers. By doing so, the assessment of the VSC using FCS-MPC in the grid-forming converter is accomplished and the following results have been achieved:

- ☐ FCS-MPC has many ways to improve the power quality in the stand-alone or grid-connected systems. One method has been proposed in this work.
- ☐ FCS-MPC has a comparable performance with several classical controllers.
- ☐ FCS-MPC is a flexible controller, which can handle multi-objective in its optimization unit without the need of several complex control blocks.
- ☐ The switching frequency variation, which is introduced by FCS-MPC, is controllable and can be fixed at different levels without using a modulator.
- ☐ The efficiency of the FCS-MPC can be improved by using an improved scheme, which optimizes the output actuation by solving an online optimization problem.
- ☐ FCS-MPC and especially the improved scheme is very robust to the parameters mismatch. The performance has been tested up to 50% change in the line impedance.

Chapter 4

Shunt Active Power Filter

As discussed in the previous chapter, model predictive control has good adaptability and robustness with simple implementation. Also, it has excellent performance during the dynamic changes. Therefore, in this chapter, a new control structure of shunt active power filter (SAPF) based on a single objective CF and using FCS-MPC scheme is introduced to compensate harmonics and also unbalanced voltages. The control structure has been compared to one of the classical strategies, which is based on space vector control.

4.1 Background

The produced harmonics by nonlinear loads have caused many power quality problems. They introduce power factor degradation, which impairs the performance of a power system, and they also produce other severe issues such as capacitor blowing, failures of sensitive devices, measurement errors in equipment, and equipment overheating. Therefore, it is mentioned in different standards that the harmonic content should be below certain limits and that is based on the considered application. In the traditional systems, passive harmonic filters are employed as the main filtering component in order to provide a clean sinusoidal output waveform. Due to their weaknesses either in bulk sizes or limited/fixed mitigation abilities, an efficient harmonic mitigation technique, shown in Fig. 4.1 is developed to replace the passive filters, and it is known as a shunt active power filter (SAPF). In [44, 54–59], various studies have surveyed and reviewed SAPFs from different perspectives such as harmonic mitigation approaches, control algorithms, and also specific applications. Different control algorithms of SAPFs are presented in [57], where the current reference following techniques, dc-link voltage reg-

ulation, and instantaneous power are examined and discussed. As discussed in [60–64], SAPFs are the most suitable devices to deal with harmonic current distortion as well as improving the total power factor performance by reducing the reactive power burden on the power system.

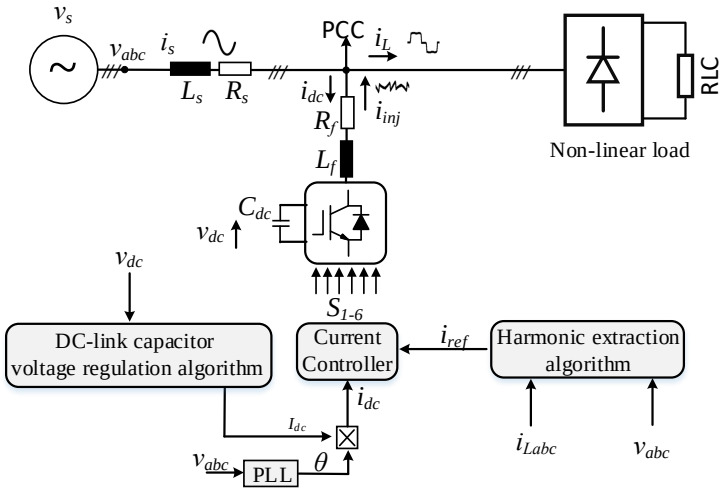

Fig. 4.1: General power circuit and control structure of a shunt active power filter (SAPF).

While the harmonics and unbalanced voltages adversely affect the operation of the grid, fast dynamics is a mandatory requirement in SAPF to protect the power system, and that represents a challenging control issue [65, 66]. In such cases, a high control bandwidth is required, and this leads to a high sampling frequency. Using the classical PI controllers may partially fail to suppress the necessary disturbances [63]. Proportional integrator (PI) controllers in a stationary reference frame almost were unable to eliminate the steady-state error and achieve satisfactory tracking performance of the desired reference [44, 56, 60]. PI and also proportional resonant (PR) controllers are sensitive to disturbances and need quite an effort, particularly in the case of the unbalanced grid, often solved by adding more controller blocks. As a result, tuning the controller becomes an extra burden.

Model predictive control has good adaptability and robustness with simple implementation [28, 31, 34, 36, 67]. Therefore, a new control structure of SAPF based on FCS-MPC scheme is introduced to control the SAPF to compensate harmonics and unbalanced voltages. Moreover, the control structure has been compared to a benchmark active filter system, which is based on space vector control. In this work, A SAPF is realized by connecting a VSC to the ac grid through filter inductor in a rectifier configuration. In the following, the conventional and proposed control structures of such configuration are discussed and investigated.

4.2 Conventional control techniques for SAPF

The benchmark system structure consists of four control stages, namely, harmonics extraction algorithm, dc-link voltage regulation based on PI controller, power converter control based on SVM, and a PLL circuit [45, 57, 63]. The SAPF controller determines the compensating current reference in real time. In that way, the SAPF can compensate for the harmonic current of a selected nonlinear load and continuously track the change in its harmonics contents. Then, a proper actuation is given to the power converter. Normally the switching frequency f_{sw} should be $>f_{hmax}$, where f_{hmax} represents the frequency of the highest order of harmonics current. In order to ensure the storage capability of SAPFs, they are connected to a capacitor on the dc side. Moreover, a low pass filter (LPF) is used to separate the average and oscil-

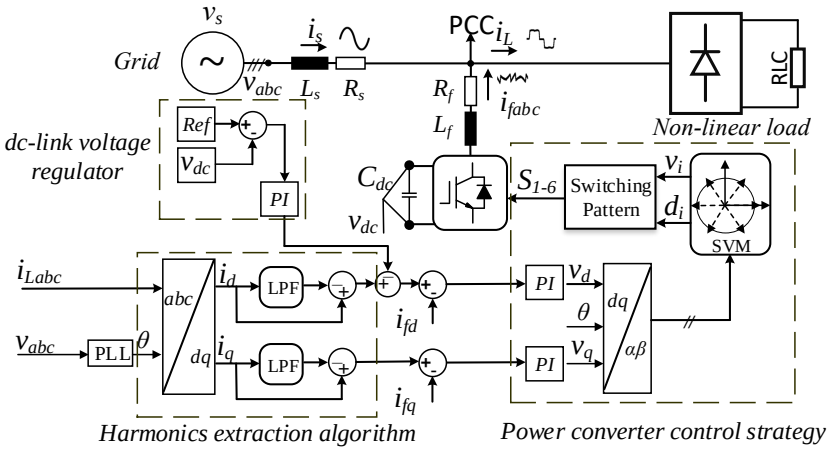

Fig. 4.2: The classical control structure used in a shunt active power filter (SAPF).

latory dq components. The oscillatory $\tilde{dq}$ components are filtered, and only the average $\bar{dq}$ components are compared with the measured filter currents i_f as it can be seen from Fig. 4.2, which depicts the overall control structure. The key idea from having space vector control as a benchmark is based on the fact that the VSC possible switching states are finite. The control strategy uses the reference voltage vector to identify the sector and calculates the switching time of the pulses. Also, space vector control of the three-phase quantities is represented as vectors in a two-dimensional $\alpha\beta$ plan, which is very similar to the predictive control strategy.

4.3 Proposed control structure for SAPF

In the discussed configuration, SAPF is able to produce any set of balanced currents and thereby compensates the reactive power and current harmonics drawn by nonlinear loads. Therefore, the SAPF filtering capabilities are limited by the control bandwidth and VSC-rated power. Hence, a new control structure which has a similar configuration to the space vector control structure is presented in this Section. The new control structure utilized predictive control as a current regulation approach. As shown in Fig. 4.3, the harmonic extraction stage still has a PLL circuit, which is used to calculate the phase angle of the grid voltage. Besides, a low pass filter is designed to separate the average and oscillatory components of the i_d and i_q as follows:

$$\begin{aligned} i_d &= \bar{i_d} + \widetilde{i_d} \\ i_q &= \bar{i_q} + \widetilde{i_q} \end{aligned} \tag{4.1}$$

Where $\bar{i_{dq}}$ are the average values and $\widetilde{i_{dq}}$ are the oscillatory parts. In this proposal, the dc-link voltage is obtained based on the ac currents and at the k^{th} instant it will be written as:

$$v_{dc}^{p}\left(k+1\right) = v_{dc}(k) + \frac{\mathrm{T_s}}{\mathrm{C_{dc}}} h_1 S(k) i_{f\alpha}(k) + \frac{\mathrm{T_s}}{\mathrm{C_{dc}}} h_2 S(k) i_{f\beta}(k). \tag{4.2}$$

Where $S(k) = [S_a(k)\ S_b(k)\ S_c(k)]^T$, $h_1 = [1\ \ 0\ \ -1]$, $h_2 = [0\ \ 1\ \ -1]$. T_s and C_{dc} are the sampling time and dc capacitor, respectively. Accordingly, this method introduces fast dynamic performance as well as it eliminates the dc voltage regulator, which is based on the PI controller. In the proposed control structure, the predictive algorithm is using a single objective cost function in order to predict the filter currents to evaluate the error and avoid a tuning process as follows:

$$g = (i_{f\alpha}^{*} - i_{f\alpha}^{p}(k+1))^2 + (i_{f\beta}^{*} - i_{f\beta}^{p}(k+1))^2. \tag{4.3}$$

Where $i_{f\alpha\beta}^{*}$ are the reference currents and $i_{f\alpha\beta}^{p}(k+1)$ are the predicted currents. In that way, superior performance can be achieved with less complex implementation. The proposed solution is using a positive and negative sequence detection strategy embedded with the MPC control unit in the discussed configuration. The positive and negative detection strategy is based on Fourier analysis. A Fourier analysis is first applied to the three input signals (v_a, v_b, v_c) and for a specified fundamental frequency, it evaluates the phasor values of the voltages. Then the transformation is applied to obtain the positive sequence, negative sequence, and zero sequences as given:

$$
\begin{aligned}
v_P &= \frac{1}{3}(v_a + a v_b + a^2 v_c) \\
v_N &= \frac{1}{3}(v_a + a^2 v_b + a v_c) \\
v_0 &= \frac{1}{3}(v_a + v_b + v_c)
\end{aligned} \tag{4.4}
$$

where v_a, v_b, v_c are the voltage phasors at a specified frequency and $a = e^{(j2\pi/3)}$. The measured grid voltages are decomposed into a positive and negative sequence. By using the MPC control unit, the supply current i_s is balanced and with less harmonics distortion than the classical strategy. Therefore, in order to validate the performance of the proposed control algorithm, up to 10% unbalance was considered [65][1].

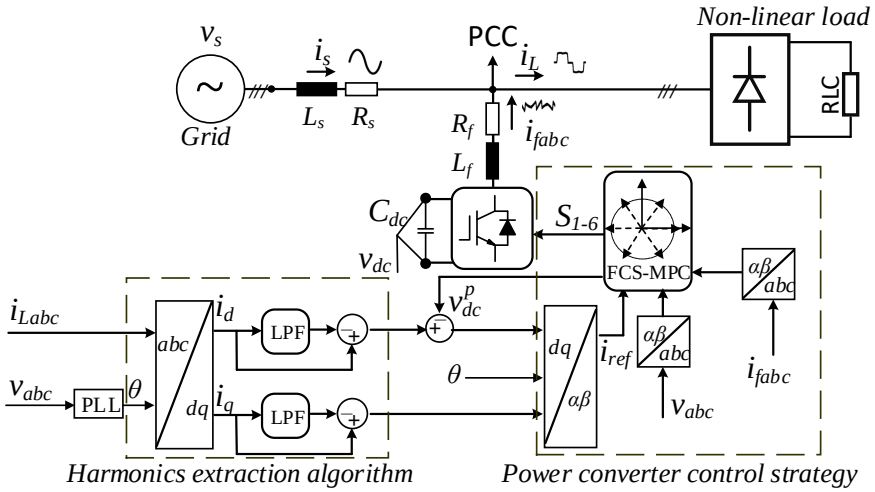

Fig. 4.3: The proposed FCS-MPC control algorithm for a shunt active power filter (SAPF).

4.4 Performance of the SAPF utilizing the proposed predictive control

A 15 kVA rated power system has been used experimentally to investigate the performance of the proposed control strategy compared to the SVPWM strategy. A three-phase diode bridge rectifier connected to resistive load has been used as a nonlinear load in order to create a distorted grid current using a standard three-phase 50 Hz grid frequency and 230 V_{rms}. The AC side is

[1]Undefined variables in this section and the previous one can be found in J2.

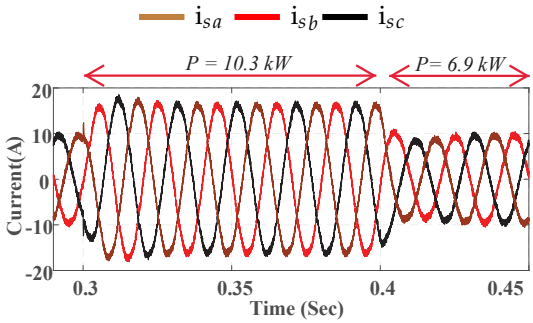

(a) MPC based.

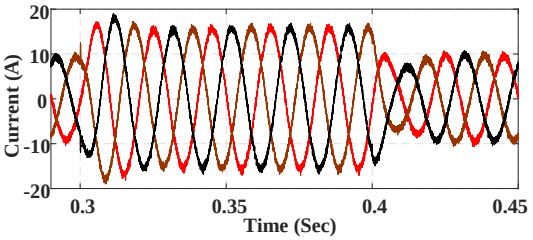

(b) SVM based.

Fig. 4.4: The simulated three-phase supply currents for the classical and proposed control algorithms, where the figures are showing the steady-state and transient operation ranging from 46% to 69% step load. (a) Supply currents using the proposed control structure while the grid voltage is balanced; and (b) supply currents using SVM while the grid voltage is balanced.

connected to the mains point at the common coupling (PCC) using a three-phase inductive filter, which has an equivalent series parameters of L_f = 5 mH and R_f = 0.4 Ω. Experimentally, the computational delay of *Ts* is needed to be compensated [68]. Table 4.1 and [J2] illustrate all the parameters used in the experimental test.

Tests have been done at a rated power equal to 46% of the power filter full capacity. Firstly, a load step has been performed and it was from a 46% to 69% of the full power, as shown in Fig. 4.4. The results show a reduction of total harmonic distortion (THDi) from THD > 28% to THD < 3.6% at 10.3 kW, where the THDi is calculated up to the 40th harmonic (2 kHz) as mentioned in [J2]. The test shows how fast the proposed control structure in harmonics compensation compared to the classical method. That was realized by both step-up and step- down tests. As mentioned before, in the proposed control structure, there is no need to provide a reference dc voltage to regulate the dc-link voltage. Results in Fig. 4.5 shows that the capacitor voltage regulation capability has been tested by stepping up and down the rectifier load. Some other results which are reported in [J2], presenting a natural decoupling be-

Table 4.1: System parameters used in the simulation and experimental SAPF setup.

Parameter	Quantity
S	15 kVA
V_{oL-L}	400 V
V_{grid}	230 V_{rms}
V_{dc}	700 V
Line frequency (f_g)	50 Hz
Sampling frequency (f_s)	50 kHz
Switching frequency (f_{swSVM})	10 kHz
Switching frequency ($f_{swavMPC}$)	$\approx$ 10 kHz
L_f	5 mH
Non-linear load	Diode rectifier and R = 60 Ω

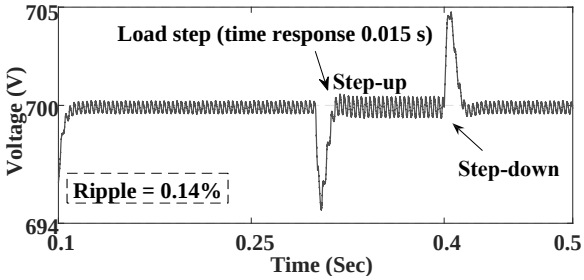

(a) Time response of the proposed control structure of both step-up and step-down load changes.

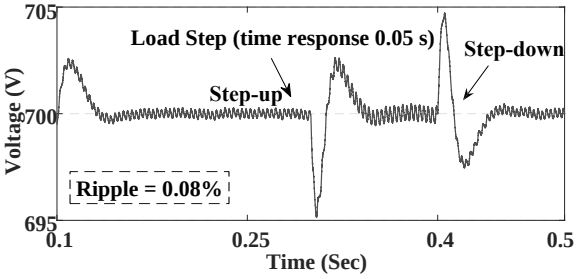

(b) Time response of the conventional SVPWM control structure of both step-up and step-down load changes.

Fig. 4.5: Capacitor voltage during the steady-state and transient operations for both classical and proposed controllers.

haviour of the predicted currents in $\alpha\beta$ frame during the transients using the FCS-MPC algorithm. It is worth to mention that the MPC requires a higher sampling frequency compared to the SVM control approach to obtain a similar average switching frequency. On the other hand, the frequency analysis which is shown in Fig. 4.6 investigates the performance of the filtered current by using classical and proposed structures. These results and discussion confirm the validity of the proposed solution and the viability of the FCS-MPC for SAPF, employing a single and compact control loop that regulates all system relevant quantities without spending effort tuning the weighting factors. Also, it shows comparative results in terms of THDi and dynamic response.

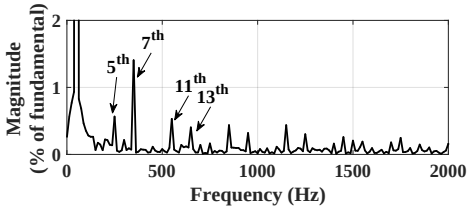

(a) Measured spectrum of (i_{sa}) using the proposed control structure.

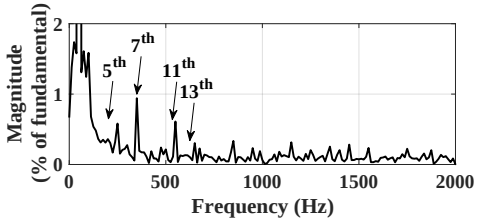

(b) Measured spectrum of (i_{sa}) using the conventional control structure.

Fig. 4.6: Frequency analysis of the current using the conventional and proposed control schemes while the grid voltage is balanced.

4.5 Voltage unbalance compensation

Using the proposed MPC control structure with the embedded sequence components extraction allows the compensation of the unbalanced grid voltage. In that way, the proposed control structure does not need a positive and negative control loop to decouple the dq components, as it can be seen in Fig. 4.7, which is implemented in the SVM control. Therefore, the proposed control structure is less complicated than the conventional SVM control structure. In Figs. 4.8, 4.9 and 4.10, comparative simulation results for voltage unbalance compensation are shown and the THDi_s for each case is re-

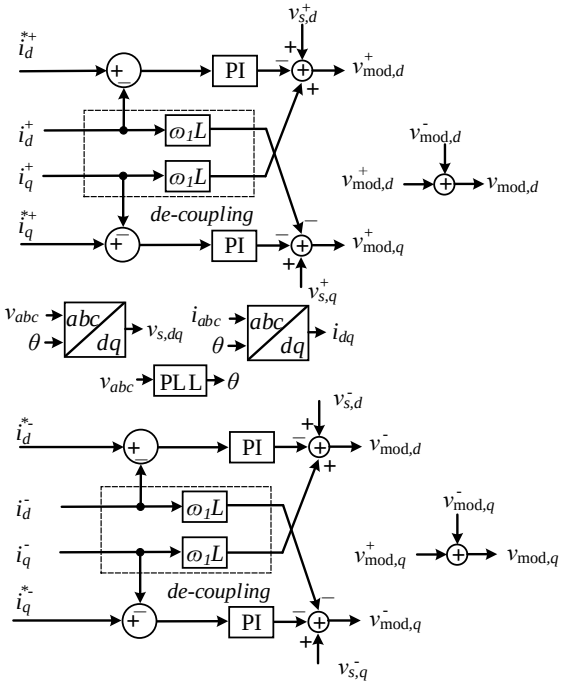

Fig. 4.7: Voltage unbalance compensation based on positive and negative sequence control used for SAPF deployed for the classical current control.

ported. Fig. 4.11 shows measurements of the proposed control structure performance in compensating the unbalance grid voltage. Figs. 4.12 to 4.15 show the frequency analysis of different cases under voltage unbalances where the amount of voltage unbalances has been calculated following IEC61000-2-2 in a three-phase system as:

$$v_{unbalanced}(\%) = \sqrt{\frac{6 \times (v_{ab}^2 + v_{bc}^2 + v_{ca}^2)}{(v_{ab} + v_{bc} + v_{ca})^2} - 2} \tag{4.5}$$

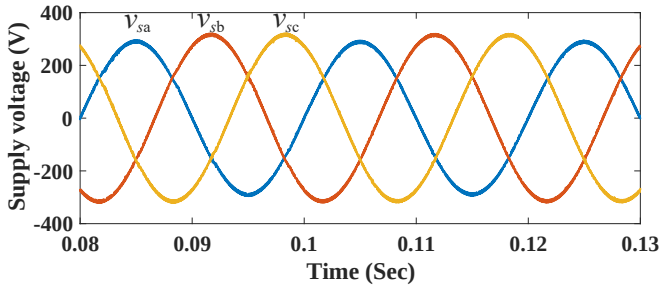

(a) 3% grid voltage unbalance (v_{sa}) following IEC 61000-2-2.

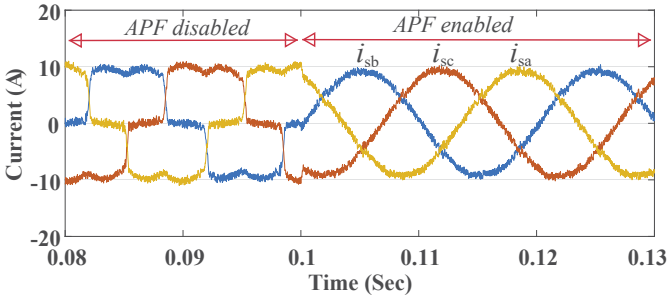

(b) Calculated THDi for phase a = 5.16%.

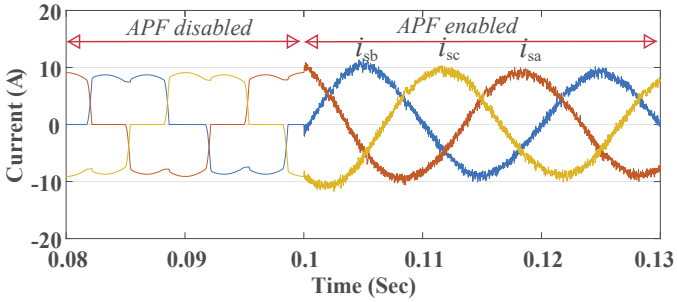

(c) Calculated THDi for phase a = 6.49%.

Fig. 4.8: Simulation results: harmonics and unbalance compensation using the proposed and classical control structure. (a) 3% grid voltage unbalance; (b) compensation in case of grid voltage unbalance using FCS-MPC, and (c) compensation in case of grid voltage unbalance using classical SVM.

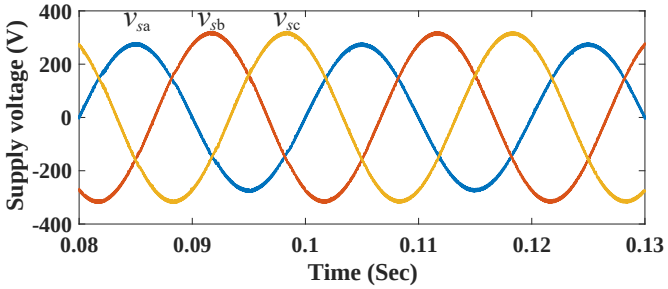

(a) 5% grid voltage unbalance (v_{sa}) following IEC 61000-2-2.

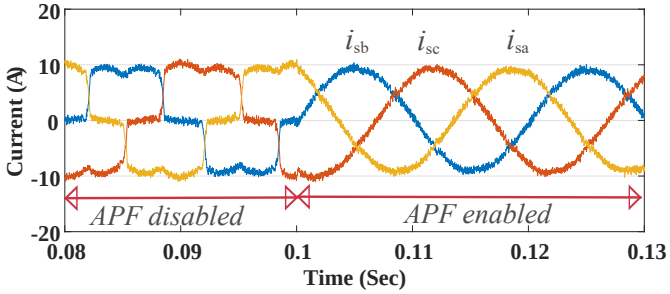

(b) Calculated THDi for phase a = 5.7%.

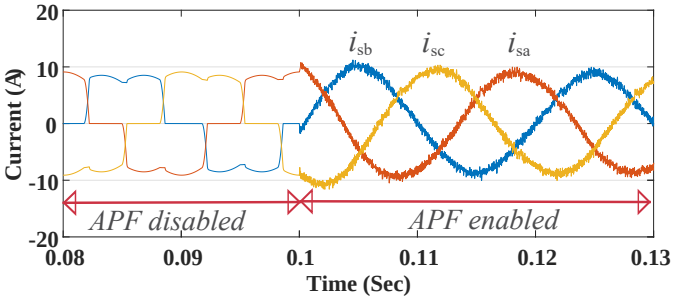

(c) Calculated THDi for phase a = 6.91%.

Fig. 4.9: Simulation results: harmonics and unbalance compensation using the proposed and classical control structure. (a) 5% grid voltage unbalance; (b) compensation in case of grid voltage unbalance using FCS-MPC, and (c) compensation in case of grid voltage unbalance using classical SVM.

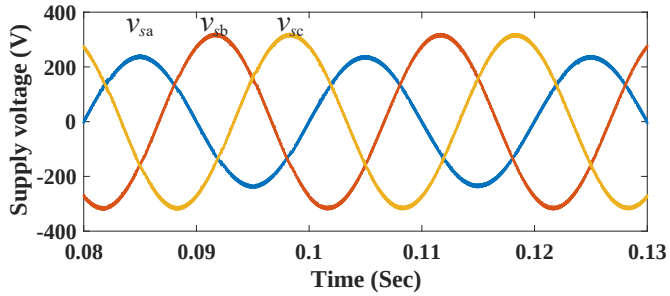

(a) 10% grid voltage unbalance (v_{sa}) following IEC 61000-2-2.

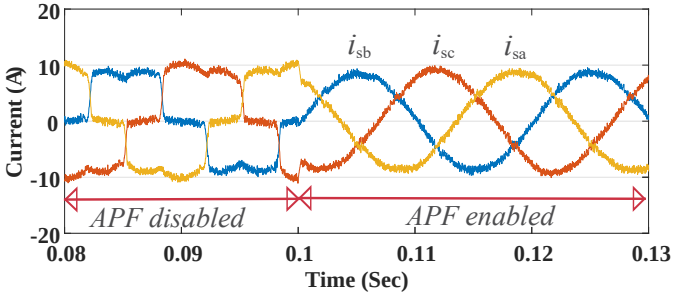

(b) Calculated THDi for phase a = 6.11%.

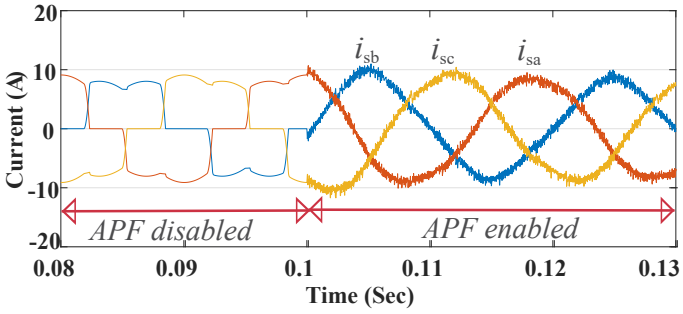

(c) Calculated THDi for phase a = 8.63%.

Fig. 4.10: Simulation results: harmonics and unbalance compensation using the proposed and classical control structure. (a) 10% grid voltage unbalance; (b) compensation in case of grid voltage unbalance using FCS-MPC, and (c) compensation in case of grid voltage unbalance using classical SVM.

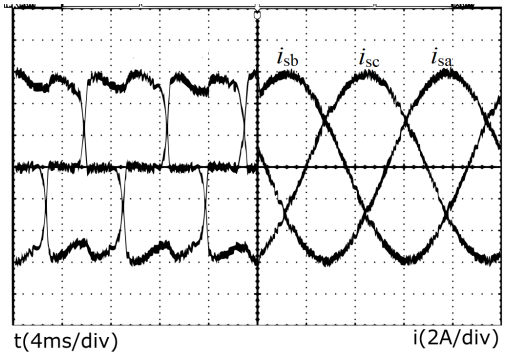

(a) 3% grid voltage unbalance

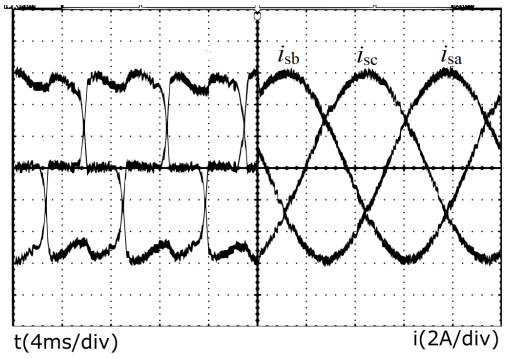

(b) 3% grid voltage unbalance

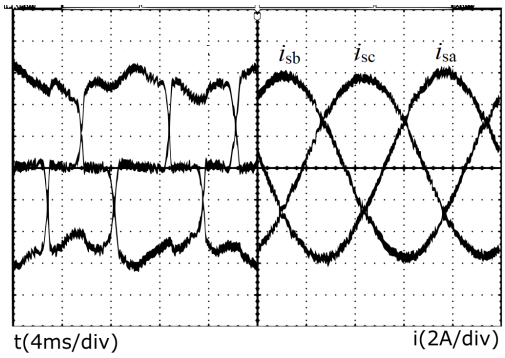

(c) 10% grid voltage unbalance

Fig. 4.11: Experimental results: harmonics and unbalance compensation using the proposed control structure in three different cases to validate the developed method. (a) compensation in case of 3 % grid voltage unbalance; (b) compensation in case of 5 % grid voltage unbalance; and (c) compensation in case of 10 % grid voltage unbalance.

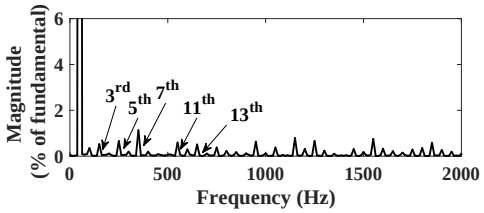

(a) Measured spectrum of (i_{sa}) using the proposed control structure.

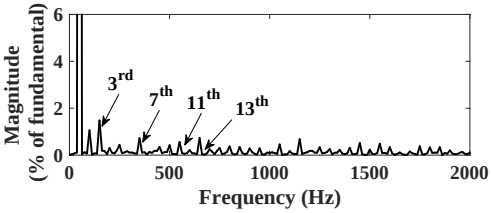

(b) Measured spectrum of (i_{sa}) using the conventional control structure.

Fig. 4.12: Case 1: frequency analysis of the current in case of 3% unbalanced grid voltage using the conventional and proposed control schemes.

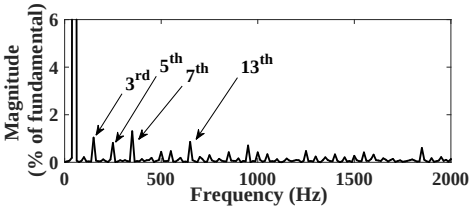

(a) Measured spectrum of (i_{sa}) using the proposed control structure.

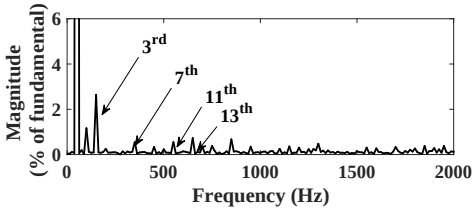

(b) Measured spectrum of (i_{sa}) using the conventional control structure.

Fig. 4.13: Case 2: frequency analysis of the current in case of 5% unbalanced grid voltage using the conventional and proposed control schemes.

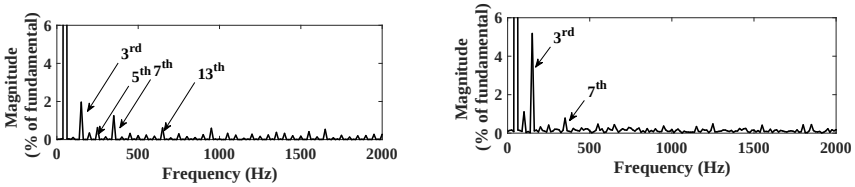

(a) Measured spectrum of (i_{sa}) using the proposed control structure.

(b) Measured spectrum of (i_{sa}) using the conventional control structure.

Fig. 4.14: Case 3: frequency analysis of the current in case of 10% unbalanced grid voltage using the conventional and proposed control schemes.

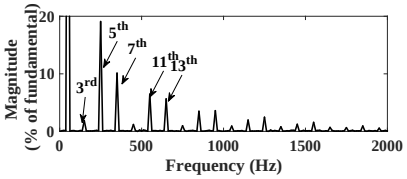

(a) Measured spectrum of (i_{sa}) in the case of 3% unbalance voltage.

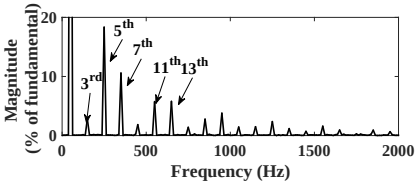

(b) Measured spectrum of (i_{sa}) in the case of 5% unbalance voltage.

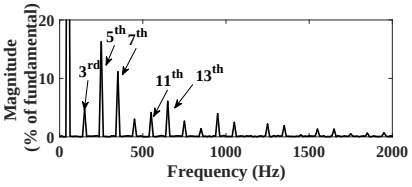

(c) Measured spectrum of (i_{sa}) in the case of 10% unbalance voltage.

Fig. 4.15: Frequency analysis of the current in case of 3%, 5%, and 10% unbalanced grid voltages where the SAPF is deactivated.

4.6 Summary

In this chapter, a new control structure for SAPF based on single objective FCS-MPC is proposed, validated, and compared to a classical control method. The single objective cost function saves the tuning effort and enables the power filter to work in a wide operation range. In the new control structure, the PI controller for the dc-link voltage regulation is eliminated, and the v_{dc} is obtained based on the ac converter currents. Compared to the conventional method, the proposed control structure has a less complicated structure and faster response. The frequency analysis of balanced and unbalanced grid voltage has been shown. The THDi report showed that the proposed control structure can provide less distortion than the classical method. Worth to mention that the sampling frequency of the proposed control structure is much higher than the classical method in order to obtain average switching frequency equal to the SVM switching frequency.

Chapter 5

Parallel Operation of VSC In MG Applications

This chapter introduces a single step prediction horizon FCS-MPC to solve the control challenges of paralleled VSCs in an AC MG environment. In order to achieve an accurate power sharing among DGs as well as voltage and frequency stability, a distinct control structure has been introduced. This chapter shows the transient improvement of multiple FCS-MPC regulated VSCs and also mitigation of the circulating power between power converters by using the improved FCS-MPC. The connection of numerous FCS-MPC regulated VSCs is based on distributed secondary control level.

5.1 Background and challenges

The coordination of different VSC units, which are used to fulfil different source/load requirements, either in grid-connected [69] or in islanded mode [70] is essential in order to meet the increasing demand for the electricity [71]. Hence, it is very important to optimize their parallel operation through different control techniques such as deadbeat control [71], cascaded linear control [72] and predictive control [70, 71, 73]. Recently, predictive control covers a wide range of controllers that have been found to control power converters.

In MGs, DGs are classified into three main categories based on their functionalities. Firstly, DGs where they are responsible for forming the grid voltage, and they are called grid-forming DGs. Secondly, DGs where they can follow up the phase angle and grid frequency to supply the desired power into the grid and they are called grid-feeding DGs. Finally, DGs where they can support the voltage and frequency of the network, as well as generate the

reference active and reactive power, they are called grid-supporting converters. In parallel and isolated operation, MGs need at least a grid-forming or grid-supporting DG combined with grid-feeding converters in order to provide the grid voltage. Using the droop approaches in the islanded mode has enabled the power sharing among the DGs according to the corresponding droop gains. Several control techniques have been proposed for the proper functioning of the parallel-connected VSCs in an MG [74–76]. MGs have frequent load changing during normal operating conditions. Therefore, DGs must respond very fast in order to achieve an efficient and reliable operation. As a result, the DG controller should be dynamic to the disturbances by including proper control objectives in the cost function (CF). In this manner, FCS-MPC is a good solution and this is similar to have a robust design of cascaded control loops in the conventional MGs, where a traditional current control strategy is used for each DG. This control strategy has further a complex structure, as well as it also has a slow dynamic response.

In this chapter, power converters are sharing the power and feeding it to the load based on a droop control approach used as a primary control. This structure results in much faster transient response and improves the robustness towards parameter variation as well as it mitigates the circulating power. Compared to the conventional grids, which are mainly dominated by high inertia synchronous generators, MGs comprising DGs with inherent low inertia. Thus, in the islanded MG, an individual load can have a significant influence on the power balance. Hence, a high bandwidth voltage and frequency control structure and appropriate load sharing are prerequisites for efficient and stable operation of MGs. In classical control, the principal objective of the primary control level is a rigid control of DGs, which mainly comprises inner voltage/current control loops, droop control function and virtual impedance loop. In order to regulate the frequency and voltage deviations caused by the operation of the primary control stage, a secondary control stage is used. The infrastructure of a conventional secondary control stage consists of a central processing unit, low bandwidth frequency and voltage regulation control loops, and a lower bandwidth communication network for sharing control signals. In the following Sections, more details for the conventional grid structure control are presented, and a distinct grid structure control is proposed and discussed.

5.2 The conventional control structure in existing MGs.

As it can be seen in Fig. 5.1, current and voltage control loops are describing the inner controllers [77]. Consequently, a droop characteristic methodology is implemented to share power among VSCs and ensure accuracy. If VSCs are considered as an ac source with an amplitude of V_i and power angle of δ_i, then the power exchange (active/reactive) between the VSC and AC bus

can be formulated as follows:

$$V_{MG} I^{ref}_{i=1,2,...,N} = \frac{V_{MG} V_{i=1,2,...,N} \angle \theta - \delta_{i=1,2,...,N}}{Z} - \frac{V^2_{MG} \angle \theta}{Z}. \tag{5.1}$$

Where $V_{MG} \angle 0$ refers to MG common bus voltage and the connected impedance is $Z_{L_i} \angle \theta_i$. Therefore, the active and reactive power exchange can be achieved from (5.2) and (5.3) respectively by:

$$P = \frac{V_{MG} V_{i=1,2,...,N}}{Z_{L_{i=1,2,...,N}}} \cos(\theta - \delta_{i=1,2,...,N}) - \frac{V^2_{MG}}{Z_{L_{i=1,2,...,N}}} cos(\theta), \tag{5.2}$$

$$Q = \frac{V_{MG} V_{i=1,2,...,N}}{Z_{L_{i=1,2,...,N}}} \sin(\theta - \delta_{i=1,2,...,N}) - \frac{V^2_{MG}}{Z_{L_{i=1,2,...,N}}} sin(\theta_{i=1,2,...,N}). \tag{5.3}$$

The droop control has a different setting and characteristics according to the line impedance, which is either resistive or inductive [C1]. The value of virtual impedance does not depend on the nonlinear load and frequency changes [78]. Thus, in resistive systems, active and reactive power exchange can be controlled based on the Q/ω and P/V droop control characteristics. Consequently, (5.2) and (5.3) can be simplified to:

$$\mathrm{V} - \mathrm{V}_o = \text{-}\mathrm{k}_p(\mathrm{P} - \mathrm{P}_o) \tag{5.4}$$

$$\mathrm{f} - \mathrm{f}_o = \mathrm{k}_q(\mathrm{Q} - \mathrm{Q}_o) \tag{5.5}$$

where f-f_o the grid frequency deviation and can be compensated by the variation of the reactive power. $V - V_o$ represents the voltage deviation and can be compensated by the active power variation $Q - Q_o$. It worth to be mentioned that the control actions can be set by the k_p and k_q parameters. Accordingly, the active and reactive power of each converter will be adjusted based on its P/V and Q/f droop characteristics to regulate the frequency and voltage, respectively.

In the conventional secondary control stage, the line frequency of an MG and voltage of each VSC are compared with the reference values. Accordingly, proper actuations are sent to the VSC in order to compensate for voltage and frequency deviations. This means that a low bandwidth communication link in the conventional structure is used in secondary control. In the conventional cascaded linear control structure, the calculated power in the inner loop should be processed through low-pass filters using lower bandwidth than internal loops. This inherent filtering stage limits the secondary control stage bandwidth, and it also leads to a slow response time during load changes.

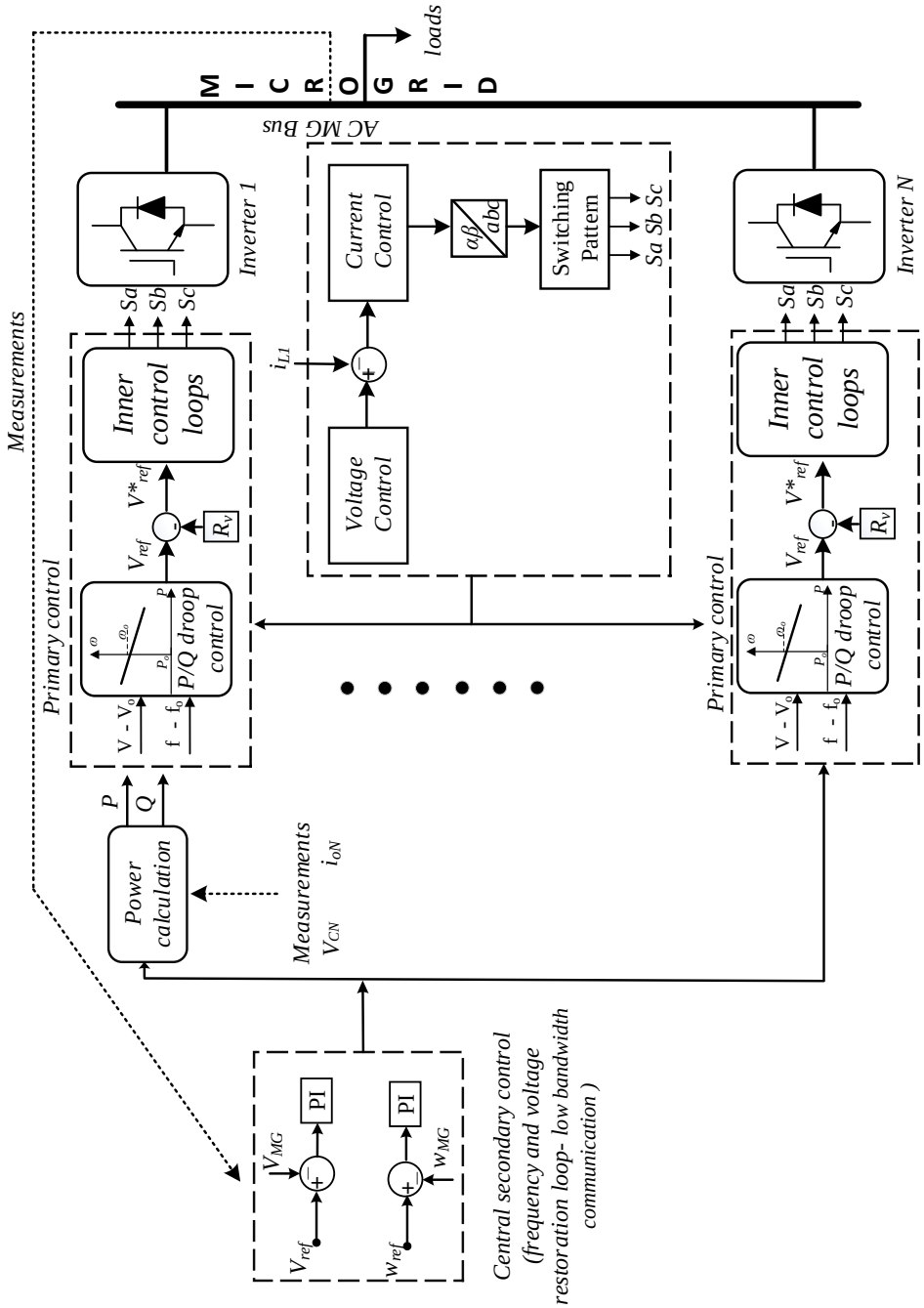

Fig. 5.1: Conventional central control structure in AC MGs.

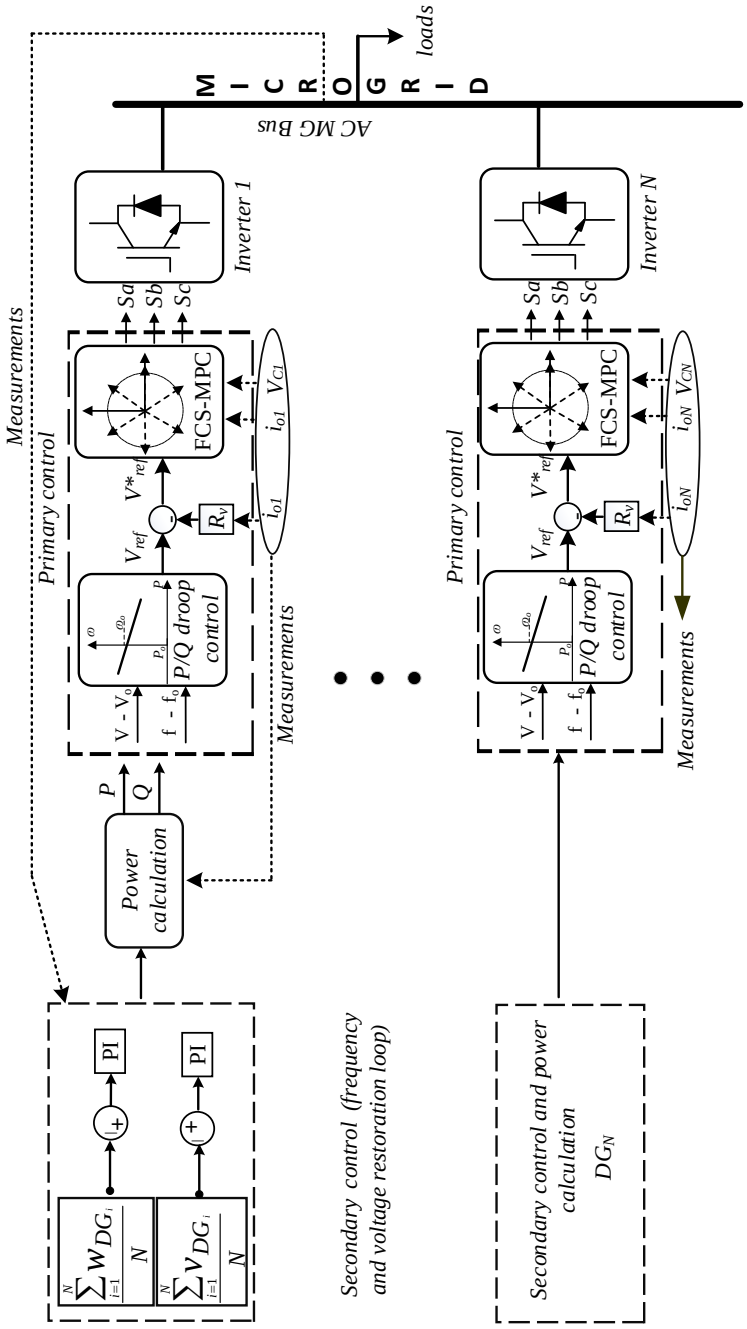

Fig. 5.2: Proposed distributed control structure in AC MGs.

5.3 The proposed structure of the MG entity based on predictive control

As it can be seen in Fig. 5.2, the primary and secondary control stages are used together as a local controller. By replacing the cascaded linear controller with FCS-MPC, the inner current/voltage control loops are eliminated. Thus, frequency and voltage regulation are achieved at the upper bandwidth limits. The FCS-MPC algorithm was explained in details in Chapter 2.

The proposed MG structure is based on the distributed secondary control, where each DG collects all measured data from the respecting converter. Then, the data are averaged, and secondary control level is responsible for sending a proper signal to the primary control level, where a frequency compensator signal can be achieved from (5.6):

$$\delta_{\omega_{DG_{i=1,2,....,N}}} = k_{p_\omega}(\omega_{ref} - \overline{\omega}_{DG_{i=1,2,....,N}}) + k_{q_\omega}\int(\omega_{ref} - \overline{\omega}_{DG_{i=1,2,....,N}})dt, \quad (5.6)$$

$$\overline{\omega}_{DG_k} = \frac{\sum_{i=1}^{N}\omega_{DG_i}}{N}, \quad (5.7)$$

where $\overline{\omega}_{DG_{i=1,2,....,N}}$ and ω_{ref} are the average of each average DG frequency and reference frequency of MG, respectively. $\delta_{\omega_{DG_{i=1,2,....,N}}}$ is a regulating signal sent from the local secondary control level to the primary control level in every sampling period, while N is the number of DGs. Similarly, the voltage signal should be sent from the secondary level to compensate for the voltage deviations caused by the primary control level.

$$\delta_{V_{DG_k}} = k_{p_V}(V_{ref} - \overline{V}_{DG_k}) + k_{i_V}\int(V_{ref} - \overline{V}_{DG_k})dt, \quad (5.8)$$

$$\overline{V}_{DG_k} = \frac{\sum_{i=1}^{N}V_{DG_i}}{N}, \quad (5.9)$$

where $\overline{V}_{DG_k}$ refers to voltages average from each converter in every sampling time. Then, signals are sent to the P/V and Q/ω primary droop control.

5.4 Transient performance

Fig. 5.2 shows the proposed structure of a microgrid system, where two inverters are connected in parallel. Both inverters are regulated by improved FCS-MPC, which is discussed in Chapter 2. The proposed structure plays an essential role in grid supporting functions, and it uses the parameters, which

Table 5.1: Parameters of the three-phase VSCs used in the validation of parallel operation.

Parameter	Quantity
Converter power S	18 kVA
DC link voltage V_{dc}	300 V
LC filter	2.4 mH, 15 μF
Resistive load R	57 Ω
Lgrid L	1.8 mH
Sampling time T_s	25 μS

are specified in Table 5.1. In that case, their voltage amplitudes and frequencies are adapted online in order to ensure a proper power sharing among different power converters by using conventional droop control methodology. Figs. 5.3 and 5.4 show that the FCS-MPC regulates the power sharing of the active and reactive power using the primary control approach. Accord-

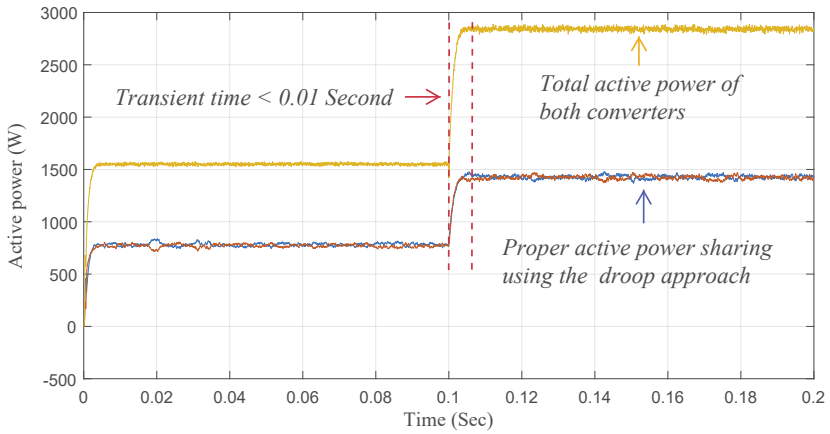

Fig. 5.3: Active power sharing and transient operation of the parallel inverters feeding an RL load.

ingly, Figs. 5.3, 5.4, 5.5, and 5.6 show that the transient time is less than 10 mS, where inverters supplying an RL load and as a result, the time will be less in case of feeding only an R load. The figures also show the accuracy of the power sharing using the droop control and virtual impedance approaches [C2].

The concept of the virtual impedance is applied to the proposed structure, where a small portion from the original voltage reference and the generated reference is sent to the FCS-MPC controller. A small R_v value has been selected based on a compromise between improving the power-sharing and keeping the voltage drop limited.

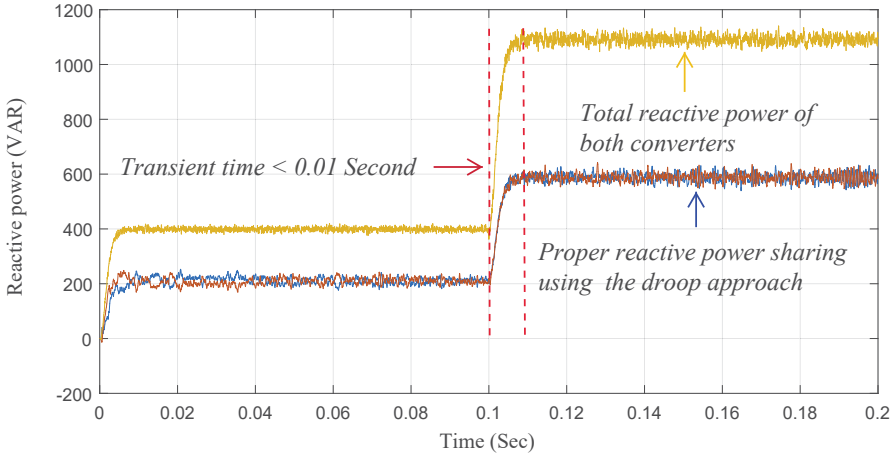

Fig. 5.4: Reactive power sharing and transient operation of the parallel inverters feeding an *RL* load.

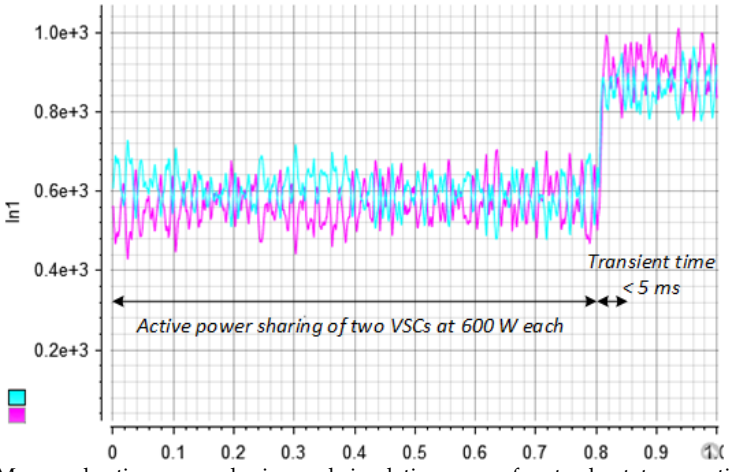

Fig. 5.5: Measured active power sharing and circulating power for steady-state operation applying the improved FCS-MPC scheme.

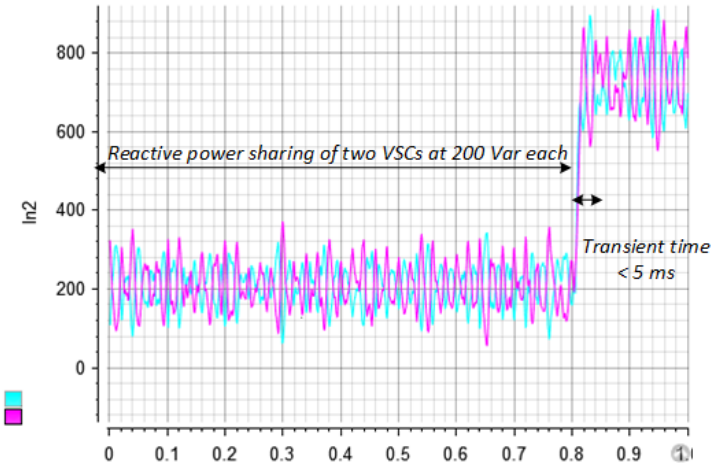

Fig. 5.6: Measured reactive power sharing and transient operation for parallel inverters feeding an *RL* load.

On the other hand, this distinct structure is very critical, especially when non-linear loads or parameters mismatch is employed. Hence, a conservative design of the droop control coefficients (K_p and K_i) can have a higher level of freedom by using the FCS-MPC.

This case study shows also circulating power impact when two parallel power converters are connected and using the improved FCS-MPC. As shown in Fig 5.7, due to the slight voltage differences in between the converters, a low circulating current is introduced. Also, the impedance of the system and the output frequency, which is determined by the droop controller, has an effect. A primary control structure with a proper tuning in the improved FCS-MPC regulated VSCs is used to ensure an improvement of the transient capabilities and as a result, the circulating power in AC MGs is reduced.

Finally, Fig. 5.8 illustrates how the proposed control structure controlled the line frequency and fastly restore it to the reference value. Figs. 5.9-5.12 show some experimental results, which further demonstrate and validate the proposed control structure.

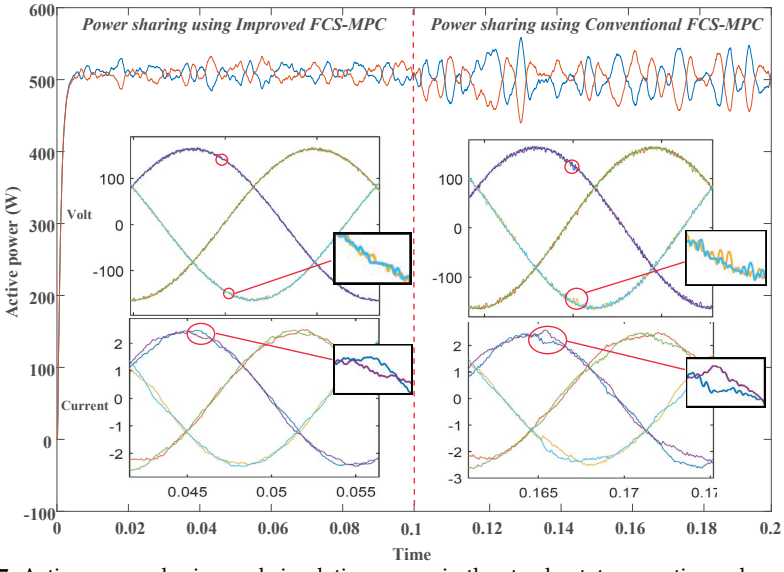

Fig. 5.7: Active power sharing and circulating power in the steady-state operation, where applying the conventional and improved FCS-MPC schemes.

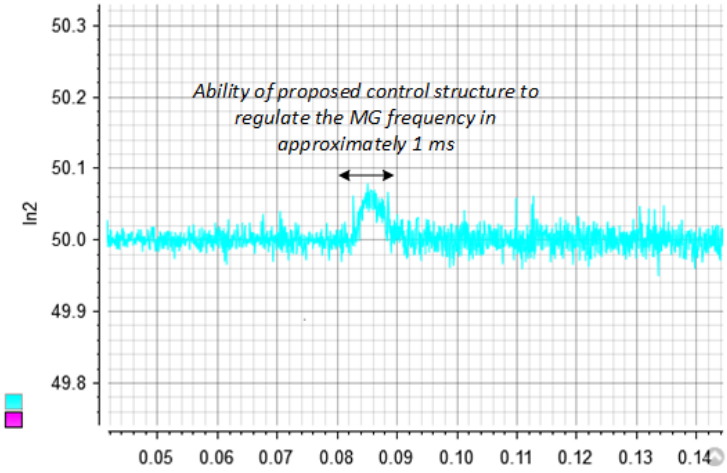

Fig. 5.8: Measured output line frequency during the transient showing fast restoration time with 100% load step.

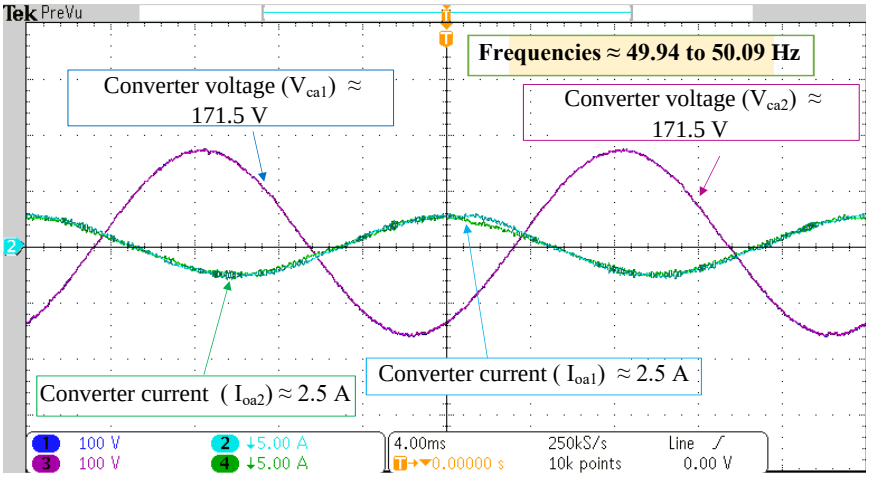

Fig. 5.9: The output voltages and currents of the VSCs regulated by FCS-MPC algorithm, where the frequency = 49.94 to 50.08 Hz and the fundamental voltage amplitude = 171.5 V.

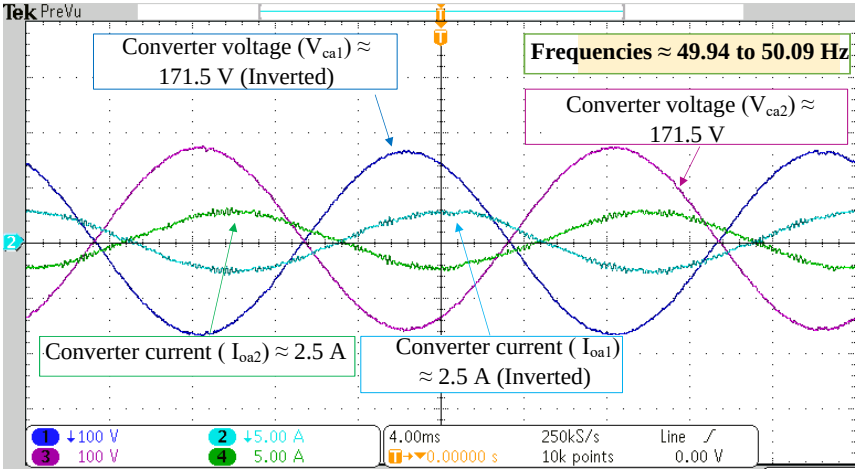

Fig. 5.10: The output voltages and currents of the VSCs regulated by FCS-MPC algorithm, where the frequency = 49.94 to 50.08 Hz and the fundamental voltage amplitude = 171.5 V (inverted).

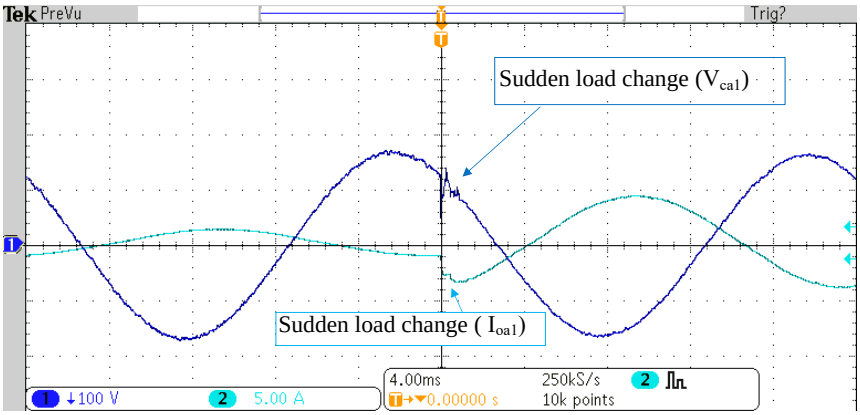

Fig. 5.11: Transient operation using one converter with 100% load step.

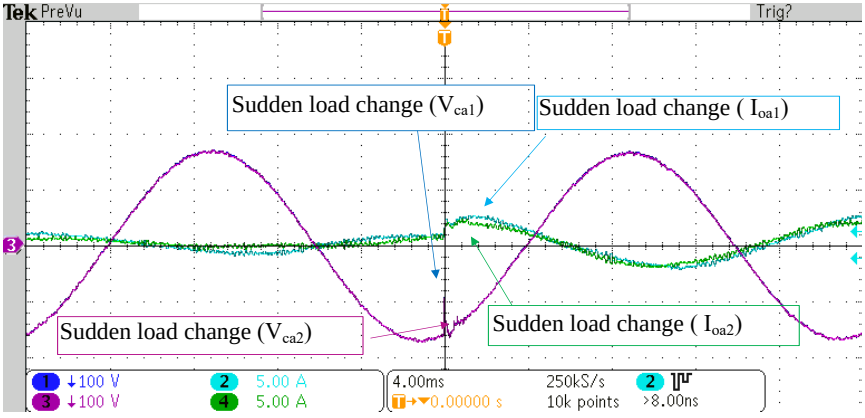

Fig. 5.12: Transient operation of both converters with 100% load step.

5.5 Summary

In this chapter, the conventional way of realizing each DG in the decentralized secondary control MG has been replaced with FCS-MPC. The new structure has given more resilience for the MG by enabling fast dynamic operations. All carried out tests have been accomplished to evaluate the transient performance for the introduced MG structure by connecting a sudden load. Experiment and simulation results have shown that the tuning of the droop characteristics ensures an excellent sharing behaviour for both steady-state and transient operations while using the FCS-MPC as the controlling unit for each DG. The results also showed how fast the regulated converters have responded to a sudden load change. This is due to the elimination of the cascaded loops for each converter in the outer control level. Finally, the employment of the improved FCS-MPC enhanced the power quality and reduced the amount of the circulating current by reducing the voltages ripples.

Chapter 6

Conclusions

This chapter summarizes the results and outcomes of the research during the Ph.D. study. The main contributions are highlighted, and the research perspectives and future works are discussed.

6.1 Summary

In this Ph.D. project, the main research focus was on several challenging issues for grid-forming converters, active power filters, and MGs by applying proper control strategies for voltage source converters. The solutions to address those issues through advancing the control structure have been proposed and discussed. In the following, a brief summary of this Ph.D. thesis is presented.

In Chapter 1, the idea behind using new control algorithms for grid-forming converters has been discussed. In the case of parallel/single converter operation, the dynamic response is one of the major concerns, which needs to be addressed. A slow response is a potential problem, which typically is related to the hierarchical nature of the conventional control strategies and may cause several challenges to the grid such as power quality degradation, efficiency, reliability concerns etc. Following the recent grid-integration requirements, a robust and fast control strategy is strongly demanded to address the adverse impact of the load variations and parameter mismatch in MG systems. The solutions to fulfil these requirements have been discussed in Chapter 2 by advancing the control of each DG in the MG. Several control solutions to predict the controlled variables during the operation of different applications have been proposed. One solution is to control each DG in the MG by an advanced FCS-MPC strategy. Another solution coordinates the control of different DG units, where the primary and secondary

control levels are improved based on the use of FCS-MPC. More solutions have been introduced for the active power filter to accomplish harmonics and unbalanced grid voltage compensation in a few milliseconds. During the Ph.D study, some concerns have been raised. One concern was related to the FCS-MPC harmonics, which is generated because of the variable switching frequency. This issue has been investigated in details in Chapter 3, where an in-depth analysis of the harmonics generated from the grid-forming converter has been carried out. By understanding the generation mechanism, it was possible to explore some solutions for this issue. Firstly, some mitigation solutions have been discussed in Chapter 3 to address this issue. Other solutions were focusing on making the switching frequency fixed and that also has been discussed in Chapter 3. Apart from harmonic challenges, reducing power loss is another aspect which is strongly demanded in the next generation of MGs. According to the discussion in Chapter 1, improving the FCS-MPC controller units introduces a high potential for a significant loss reduction compared to the conventional MPC methods. Therefore, the power losses distribution has been analyzed following a fair comparison criterion for different case studies, which is also discussed in Chapter 3. In Chapter 4, which took the active power filters into consideration, has discussed enhancements of the active filtering devices using FCS-MPC. Moreover, the impact of non-linear loads and the unbalanced grid voltage have been considered and investigated. The performance of the proposed control structure in SAPF application compared to conventional methods is another concern, which is discussed and studied. The evaluation results indicate that using conventional methods can increase the complication of the control system structure. In that case, a certain design margin in terms of simplicity, computational burden, and fast dynamic response is required to ensure high reliability and performance of the SAPF under various grid conditions.

Although the performance of the SAPFs can be strengthened by using the FCS-MPC, the control strategy of the VSC can also contribute to further improvement in MG applications. The possibility to improve the fast operation, especially during the MG transients through the control of each DG was the main research focus in Chapter 5. There, the parallel operation of two VSCs was considered, where the primary and secondary control levels were adopted. In the case of using MPC in each DG in the MG, the frequency and voltage restoration time is improved at least 10 times compared to the hierarchical conventional control methods. This contributes to the improvement in the reliability and performance of the DGs due to the reduced stress time.

6.2 Main contributions

In this part, the main contributions of this Ph.D. project based on the research outcomes are summarized as follows:

- *Improved control strategy of stand-alone and grid-connected converters*
  This Ph.D. study has proposed a new FCS-MPC control scheme to realize the power control functionality for stand-alone and grid-connected converters. Thereby, comprehensive performance analysis has been done for the conventional and improved FCS-MPC schemes utilizing a typical VSC. The proposed scheme enabled a good enhancement for the power quality by using one-step prediction. Compared to the classical MPC methods, the new scheme achieved a high power quality with less computation. Moreover, the robustness of the improved FCS-MPC has been investigated. Many analysis has been done for the proposed scheme in order to benchmarked it compared with the classical FCS-MPC method.

- *Impact of the FCS-MPC in SAPF applications*
  This Ph.D. study has proposed a new control structure for SAPF and based on predictive current control. The proposed control structure has provided a fast compensation mechanism for the distorted MGs. By proposing the new control structure, the system becomes less complex compared to classical approaches. Also, using the predictive current control scheme without weighting factor employment and based on a single objective has enabled a rapid and high performance in compensating both harmonics and unbalanced grid voltage.

- *Improved transient performance in decentralized MG structure*
  By replacing the classical and hierarchical control algorithms of each DG with an improved FCS-MPC, the distributed secondary control levels are able to compensate voltage and frequency deviations with high bandwidth and super fast response rates compared to the conventional linearized cascaded control methods. Moreover, circulating power between converters has been reduced due to the power quality enhancement, which is provided by the improved FCS-MPC scheme.

6.3 Future Work

Although several aspects of the VSCs regulated by FCS-MPC have been investigated in this Ph.D. project, there are still other challenges which need to be addressed for next-generation of MGs systems.

- In spite of that this Ph.D. project proposes several improvements for the VSCs regulated by FCS-MPC, which are used in stand-alone or in grid-connected applications, there are also other solutions to build the MGs structure. It could be more beneficial to combine different control methodologies in one MG entity. This combination will enable the MG to take advantage of each control strategy and enhance the overall MG

operation. It could also be beneficial to combine different control solutions and scale up the system with many units in order to reduce the cost while maintaining fast performance.

- For the improved FCS-MPC, it is still suffering from the process of the weighting factor tuning, which is essential to ensure high performance for operations. Therefore, a proposal to use a sequential improved FCS-MPC algorithm for grid-forming converters should be investigated and studied. Another suggestion is to use intelligent control techniques to ensure the best tuning for the weighting factor based on the operation conditions.

- There should be a standard (new indices) way to calculate the harmonics and inter-harmonics, which are generated due to the switching frequency variation of the FCS-MPC. Researchers are always pointing out the THD without considering the upper limits of the switching frequency. That also happens when different fixed switching frequency techniques are used in the FCS-MPC control unit. It would be more beneficial and logical if there is a standard way to measure all switching states precisely during the steady-state and transient operation.

- It could be interesting to investigate the reliability of the system's active and passive components using improved FCS-MPC.

- Using the periodic improved FCS-MPC results in acceptable behaviour in many aspects. It retains all the advantages of the FCS-MPC and restricts the switching frequency to the minimum possible band. Therefore, it would be an excellent idea to take the benefits of P-IMPC in designing the physical *LC* filter in an optimised way and avoid oversizing the filter.

References

[1] F. de Bosio, M. Pastorelli, L. A. d. S. Ribeiro, M. S. Lima, F. Freijedo, and J. M. Guerrero. Current control loop design and analysis based on resonant regulators for microgrid applications. *41st Annual Conference of the IEEE Industrial Electronics Society*, pages 005322–005327, Nov 2015.

[2] P. C. Loh and D. G. Holmes. Analysis of multiloop control strategies for lc/cl/lcl-filtered voltage-source and current-source inverters. *IEEE Transactions on Industry Applications*, 41(2):644–654, March 2005.

[3] M. J. Ryan, W. E. Brumsickle, and R. D. Lorenz. Control topology options for single-phase ups inverters. *IEEE Transactions on Industry Applications*, 33(2):493–501, March 1997.

[4] D. Wu, F. Tang, T. Dragicevic, J. C. Vasquez, and J. M. Guerrero. A control architecture to coordinate renewable energy sources and energy storage systems in islanded microgrids. *IEEE Transactions on Smart Grid*, 6(3):1156–1166, May 2015.

[5] D. N. Zmood, D. G. Holmes, and G. H. Bode. Frequency-domain analysis of three-phase linear current regulators. *IEEE Transactions on Industry Applications*, 37(2):601–610, March 2001.

[6] J. M. Espi Huerta, J. Castello, J. R. Fischer, and R. Garcia-Gil. A synchronous reference frame robust predictive current control for three-phase grid-connected inverters. *IEEE Transactions on Industrial Electronics*, 57(3):954–962, March 2010.

[7] P. Mattavelli. A closed-loop selective harmonic compensation for active filters. *IEEE Transactions on Industry Applications*, 37(1):81–89, Jan 2001.

[8] L. Malesani, P. Mattavelli, and S. Buso. Robust dead-beat current control for pwm rectifiers and active filters. *IEEE Transactions on Industry Applications*, 35(3):613–620, May 1999.

[9] D. P. Ariyasinghe and D. M. Vilathgamuwa. Stability analysis of microgrids with constant power loads. *IEEE International Conference on Sustainable Energy Technologies*, pages 279–284, 2008.

[10] S. Kouro, M. A. Perez, J. Rodriguez, A. M. Llor, and H. A. Young. Model predictive control: Mpc's role in the evolution of power electronics. *IEEE Industrial Electronics Magazine*, 9(4):8–21, Dec 2015.

[11] Linder, Arne, and R. Kennel. Model predictive control for electrical drives. *IEEE 36th Power Electronics Specialists Conference*, pages 1793–1799, 2005.

[12] S. Kouro, P. Cortés, René Vargas, U. Ammann, and J. Rodríguez. Model predictive control—a simple and powerful method to control power converters. *IEEE Transactions on Industrial Electronics*, 56(6):1826–1838, 2008.

[13] Linder and R. Kennel. Direct model predictive control-a new direct predictive control strategy for electrical drives. *European Conference on Power Electronics and Applications*, pages 10–pp, 2005.

[14] J. Rodríguez, J. Pontt, C. Silva, P. Cortes, U. Amman, and S. Rees. Predictive current control of a voltage source inverter. *IEEE 35th Annual Power Electronics Specialists Conference*, 3:2192–2196, 2004.

[15] R. Majumder. Some aspects of stability in microgrids. *IEEE Transactions on Power Systems*, 28(3):3243–3252, 2013.

[16] T. Dragičević. Model predictive control of power converters for robust and fast operation of ac microgrids. *IEEE Transactions on Power Electronics*, 33(7):6304–6317, 2017.

[17] S. Buso, S. Fasolo, and P. Mattavelli. Uninterruptible power supply multiloop control employing digital predictive voltage and current regulators. *IEEE Transactions on Industry Applications*, 37(6):1846–1854, Nov 2001.

[18] N. Panten, N. Hoffmann, and F. W. Fuchs. Finite control set model predictive current control for grid-connected voltage-source converters with LCL filters: a study based on different state feedbacks. *IEEE Transactions on Power Electronics*, 31(7):5189–5200, July 2016.

[19] A. M. Hava, R. J. Kerkman, and T. A. Lipo. Carrier-based pwm-vsi overmodulation strategies: analysis, comparison, and design. *IEEE Transactions on Power Electronics*, 13(4):674–689, July 1998.

[20] J. C. Vasquez, J. M. Guerrero, M. Savaghebi, J. Eloy-Garcia, and R. Teodorescu. Modeling, analysis, and design of stationary-reference-frame droop-controlled parallel three-phase voltage source inverters. *IEEE Transactions on Industrial Electronics*, 60(4):1271–1280, April 2013.

[21] F. de Bosio, L. A. de Souza Ribeiro, F. D. Freijedo, M. Pastorelli, and J. M. Guerrero. Effect of state feedback coupling and system delays on the transient performance of stand-alone vsi with lc output filter. *IEEE Transactions on Industrial Electronics*, 63(8):4909–4918, Aug 2016.

[22] J. Rodriguez and P. Cortes. Predictive control of power converters and electrical drives. *Wiley-IEEE Press, Chichester West Sussex UK, 2012*.

[23] M. Huang, F. Blaabjerg, Y. Yang, and W. Wu. Step by step design of a high order power filter for three-phase three-wire grid-connected inverter in renewable energy system. *4th IEEE International Symposium on Power Electronics for Distributed Generation Systems (PEDG)*, pages 1–8, July 2013.

[24] J. Rodriguez, J. Pontt, C. A. Silva, P. Correa, P. Lezana, P. Cortes, and U. Ammann. Predictive current control of a voltage source inverter. *IEEE Transactions on Industrial Electronics*, 54(1):495–503, Feb 2007.

[25] S. Vazquez, J. I. Leon, L. G. Franquelo, J. M. Carrasco, O. Martinez, J. Rodriguez, P. Cortes, and S. Kouro. Model predictive control with constant switching frequency using a discrete space vector modulation with virtual state vectors. *IEEE International Conference on Industrial Technology*, pages 1–6, Feb 2009.

[26] H. Young and J. Rodriguez. Comparison of finite-control-set model predictive control versus a svm-based linear controller. *15th European Conference on Power Electronics and Applications (EPE)*, pages 1–8, Sept 2013.

[27] S. Vazquez, J. I. Leon, L. G. Franquelo, J. Rodriguez, H. A. Young, A. Marquez, and P. Zanchetta. Model predictive control: a review of its applications in power electronics. *IEEE Industrial Electronics Magazine*, 8(1):16–31, March 2014.

[28] P. Cortes, G. Ortiz, J. I. Yuz, J. Rodriguez, S. Vazquez, and L. G. Franquelo. Model predictive control of an inverter with output LC filter for UPS applications. *IEEE Transactions on Industrial Electronics*, 56(6):1875–1883, June 2009.

[29] H. Han, X. Hou, J. Yang, J. Wu, M. Su, and J. M. Guerrero. Review of power sharing control strategies for islanding operation of ac microgrids. *IEEE Transactions on Smart Grid*, 7(1):200–215, Jan 2016.

[30] M. Alhasheem, T. Dragicevic, and F. Blaabjerg. Evaluation of multi predictive controllers for a two-level three-phase stand-alone voltage source converter. *IEEE Southern Power Electronics Conference*, pages 1–6, Dec 2017.

[31] P. Cortes, J. Rodriguez, S. Vazquez, and L. G. Franquelo. Predictive control of a three-phase UPS inverter using two steps prediction horizon. *IEEE International Conference on Industrial Technology*, pages 1283–1288, March 2010.

[32] J. Rodriguez, P. Cortes, R. Kennel, and M. P. Kazrnierkowski. Model predictive control – a simple and powerful method to control power

converters. *Proc. of IEEE 6th International Power Electronics and Motion Control Conference*, pages 41–49, May 2009.

[33] T. Dragicevic, M. Alhasheem, M. Lu, and F. Blaabjerg. Improved model predictive control for high voltage quality in microgrid applications. *IEEE Energy Conversion Congress and Exposition*, pages 4475–4480, Oct 2017.

[34] H. Young and J. Rodriguez. Comparison of finite-control-set model predictive control versus a svm-based linear controller. *15th European Conference on Power Electronics and Applications*, pages 1–8, Sep. 2013.

[35] M. Aguirre, S. Kouro, C. A. Rojas, J. Rodriguez, and J. I. Leon. Switching frequency regulation for fcs-mpc based on a period control approach. *IEEE Transactions on Industrial Electronics*, 65(7):5764–5773, July 2018.

[36] J. Rodriguez, J. Pontt, C. Silva, P. Cortes, U. Amman, and S. Rees. Predictive current control of a voltage source inverter. *IEEE 35th Annual Power Electronics Specialists Conference (IEEE Cat. No.04CH37551)*, 3:2192–2196 Vol.3, June 2004.

[37] M. A. Hosseinzadeh, M. Sarbanzadeh, E. Sarebanzadeh, M. Rivera, and J. Muñoz. Predictive control in power converter applications: Challenge and trends. *IEEE International Conference on Automation/XXIII Congress of the Chilean Association of Automatic Control (ICA-ACCA)*, pages 1–6, Oct 2018.

[38] S. Vazquez, J. I. Leon, L. G. Franquelo, J. Rodriguez, H. A. Young, A. Marquez, and P. Zanchetta. Model Predictive Control: A Review of Its Applications in Power Electronics. *IEEE Industrial Electronics Magazine*, 8(1):16–31, March 2014.

[39] Y. Zhang, J. Liu, and S. Fan. On the inherent relationship between finite control set model predictive control and svm-based deadbeat control for power converters. *IEEE Energy Conversion Congress and Exposition (ECCE)*, pages 4628–4633, Oct 2017.

[40] Y. Zhang, J. Liu, and S. Fan. On the inherent relationship between finite control set model predictive control and svm-based deadbeat control for power converters. *IEEE Energy Conversion Congress and Exposition (ECCE)*, pages 4628–4633, Oct 2017.

[41] F. Gavilan, D. Caballero, S. Toledo, E. Maqueda, R. Gregor, J. Rodas, M. Rivera, and I. Araujo-Vargas. Predictive power control strategy for a grid-connected 2l-vsi with fixed switching frequency. *IEEE International Autumn Meeting on Power, Electronics and Computing (ROPEC)*, pages 1–6, Nov 2016.

[42] M. Tomlinson, H. d. T. Mouton, R. Kennel, and P. Stolze. A fixed switching frequency scheme for finite control set model predictive control concept and algorithm. *IEEE Transactions on Industrial Electronics*, 63(12):7662–7670, Dec 2016.

[43] M. Rivera. Predictive current control for a vsi with reduced common mode voltage operating at fixed switching frequency. *IEEE 24th International Symposium on Industrial Electronics*, pages 980–985, June 2015.

[44] A. Renault, M. Rivera, J. Rodas, L. Comparatore, J. Pacher, and R. Gregor. Modulated model predictive current control for h-bridge two-level single phase active power filters statcom. *12th IEEE Conference on Industrial Electronics and Applications (ICIEA)*, pages 355–359, June 2017.

[45] L. Tarisciotti, A. Formentini, A. Gaeta, M. Degano, P. Zanchetta, R. Rabbeni, and M. Pucci. Model predictive control for shunt active filters with fixed switching frequency. *IEEE Transactions on Industry Applications*, 53(1):296–304, Jan 2017.

[46] B. Gadalla, E. Schaltz, Y. Siwakoti, and F. Blaabjerg. Thermal performance and efficiency investigation of conventional boost, z-source and y-source converters. In *Proc. of 2016 IEEE 16th International Conference on Environment and Electrical Engineering (EEEIC)*, pages 1–6, June 2016.

[47] A. Abdelhakim, P. Davari, F. Blaabjerg, and P. Mattavelli. Switching loss reduction in the three-phase quasi-z-source inverters utilizing modified space vector modulation strategies. *IEEE Transactions on Power Electronics*, 33(5):4045–4060, 5 2018.

[48] G.O. Cimuca, C. Saudemont, B. Robyns, and M.M. Radulescu. Control and performance evaluation of a flywheel energy-storage system associated to a variable-speed wind generator. *IEEE Transactions on Industrial Electronics*, 53(4):1074–1085, 2006.

[49] H. Kakigano, Y. Miura, and T. Ise. Low-voltage bipolar-type dc microgrid for super high quality distribution. *IEEE Transactions on Power Electronics*, 25(12):3066 –3075, dec. 2010.

[50] F. Bosio, L. A. de Souza Ribeiro, F. D. Freijedo, M. Pastorelli, and J. M. Guerrero. Effect of state feedback coupling and system delays on the transient performance of stand-alone VSI with LC output filter. *IEEE Transactions on Industrial Electronics*, 63(8):4909–4918, Aug 2016.

[51] M. P. Kazmierkowski and L. Malesani. Current control techniques for three-phase voltage-source pwm converters: a survey. *IEEE Transactions on Industrial Electronics*, 45(5):691–703, Oct 1998.

[52] V. Blasko and V. Kaura. A novel control to actively damp resonance in input lc filter of a three-phase voltage source converter. *IEEE Transactions on Industry Applications*, 33(2):542–550, 1997.

[53] J. I. Leon, S. Kouro, L. G. Franquelo, J. Rodriguez, and B. Wu. The essential role and the continuous evolution of modulation techniques for voltage-source inverters in the past, present, and future power electronics. *IEEE Transactions on Industrial Electronics*, 63(5):2688–2701, May 2016.

[54] S. P. Litran, P. Salmeron, J. R. Vazquez, R. S. Herrera, and A. Perez. Control strategy for hybrid power filter to compensate unbalanced and non-linear, three-phase loads. *13th European Conference on Power Electronics and Applications*, pages 1–10, Sep. 2009.

[55] K. Antoniewicz and M. Jasinski. Experimental comparison of hysteresis based control and finite control state set model predictive control of shunt active power filter. *Selected Problems of Electrical Engineering and Electronics (WZEE)*, pages 1–6, Sep. 2015.

[56] H. Afghoul and F. Krim. Comparison between pi and fuzzy dpc control of a shunt active power filter. *IEEE International Energy Conference and Exhibition (ENERGYCON)*, pages 146–151, Sep. 2012.

[57] Y. Hoon, M. Radzi, M. Amran, M. K. Hassan, and N. F. Mailah. Control algorithms of shunt active power filter for harmonics mitigation: A review. *Energies*, 10(12), 2017.

[58] R. Panigrahi, B. Subudhi, and P. C. Panda. Model predictive-based shunt active power filter with a new reference current estimation strategy. *IET Power Electronics*, 8(2):221–233, 2015.

[59] W. Xiao-gang, X. Yun-xiang, and S. Ding-xin. Simplified model predictive control for a shunt active power filter. *IEEE Power Electronics Specialists Conference*, pages 3279–3283, June 2008.

[60] S. Rahmani, A. Hamadi, K. Al-Haddad, and L. A. Dessaint. A combination of shunt hybrid power filter and thyristor-controlled reactor for power quality. *IEEE Transactions on Industrial Electronics*, 61(5):2152–2164, May 2014.

[61] V. K. Gonuguntala, A. Frobel, and R. Vick. Performance analysis of finite control set model predictive controlled active harmonic filter. *18th International Conference on Harmonics and Quality of Power (ICHQP)*, pages 1–6, May 2018.

[62] S. C. Ferreira, R. B. Gonzatti, R. R. Pereira, C. H. da Silva, L. E. B. da Silva, and G. Lambert-Torres. Finite control set model predictive control for dynamic reactive power compensation with hybrid active power filters. *IEEE Transactions on Industrial Electronics*, 65(3):2608–2617, March 2018.

[63] H. Akagi, E. H. Watanabe, and M. Aredes. Instantaneous power theory and applications to power conditioning. *John Wiley & Sons*, 2017.

[64] AK. Al-Othman, ME. AlSharidah, N. A Ahmed, B. N. Alajmi, et al. Model predictive control for shunt active power filter in synchronous reference frame. *J Electr Eng Technol*, 11:1921–718, 2016.

[65] H. Soltani, P. Davari, F. Blaabjerg, and F. Zare. Harmonic distortion performance of multi three-phase scr-fed drive systems with controlled dc-link current under unbalanced grid. *43rd Annual Conference of the IEEE Industrial Electronics Society*, pages 1210–1214, Oct 2017.

[66] D. Kumar, P. Davari, F. Zare, and F. Blaabjerg. Analysis of three-phase rectifier systems with controlled dc-link current under unbalanced grids. *IEEE Applied Power Electronics Conference and Exposition (APEC)*, pages 2179–2186, March 2017.

[67] M. Tomlinson, H. d. T. Mouton, R. Kennel, and P. Stolze. A fixed switching frequency scheme for finite-control-set model predictive control—concept and algorithm. *IEEE Transactions on Industrial Electronics*, 63(12):7662–7670, Dec 2016.

[68] P. Cortes, J. Rodriguez, C. Silva, and A. Flores. Delay compensation in model predictive current control of a three-phase inverter. *IEEE Transactions on Industrial Electronics*, 59(2):1323–1325, Feb 2012.

[69] F. Blaabjerg, Y. Yang, D. Yang, and X. Wang. Distributed power-generation systems and protection. *Proceedings of the IEEE*, 105(7):1311–1331, 2017.

[70] S. Kouro, P. Cortés, R. Vargas, U. Ammann, and J. Rodríguez. Model predictive control—a simple and powerful method to control power converters. *IEEE Transactions on industrial electronics*, 56(6):1826–1838, 2008.

[71] P. Mattavelli. An improved deadbeat control for ups using disturbance observers. *IEEE Transactions Industrial Electronics*, 52(1):206–212, Feb 2005.

[72] P. C. Loh and D. G. Holmes. Analysis of multiloop control strategies for lc/cl/lcl-filtered voltage-source and current-source inverters. *IEEE Transactions on Industry Applications*, 41(2):644–654, 2005.

[73] S. Buso, S. Fasolo, and P. Mattavelli. Uninterruptible power supply multiloop control employing digital predictive voltage and current regulators. *IEEE Transactions on Industry Applications*, 37(6):1846–1854, Nov 2001.

[74] J. Rocabert, A. Luna, F. Blaabjerg, and P. Rodriguez. Control of power converters in ac microgrids. *IEEE Transactions on Power Electronics*, 27(11):4734–4749, 2012.

[75] J. M. Guerrero, L. Hang, and J. Uceda Antolín. Control of distributed uninterruptible power supply systems. *IEEE Transactions on Industrial Electronics*, 55(8):2845–2859, 2008.

[76] J. Rodriguez, P. Cortes, R. Kennel, and M. P. Kazrnierkowski. Model predictive control – a simple and powerful method to control power converters. In *Proc. of IEEE 6th International Power Electronics and Motion Control Conference*, pages 41–49, May 2009.

[77] S. Anand, B. G. Fernandes, and J. Guerrero. Distributed control to ensure proportional load sharing and improve voltage regulation in low-voltage dc microgrids. *IEEE Transactions on Power Electronics*, 28(4):1900–1913, 2012.

[78] J. Schiffer, T. Seel, J. Raisch, and T. Sezi. Voltage stability and reactive power sharing in inverter-based microgrids with consensus-based distributed voltage control. *IEEE Transactions on Control Systems Technology*, 24(1):96–109, 2015.

Part II

Selected Papers

ISSN (online): 2446-1636
ISBN (online): 978-87-7210-533-8 AALBORG UNIVERSITY PRESS